Diversity and biotechnological potential of filamentous fungi isolated from sediments of Basque estuaries.

A. Otamendi[a] (ORCID: 0000-0002-1475-321X), Z. Agirrezabala[a], C. Perez-Cruz[b] (ORCID: 0000-0003-2796-5315), R. Liébana[b] (ORCID: 0000-0002-2196-5632), I. Berregi[a] (0000-0002-5567-8404), L. Alonso-Sáez[b] (0000-0003-1757-4767), MT. Dueñas[a] (0000-0001-7551-7037), A. Lanzén[c,d] (0000-0002-7138-6364), O. Etxebeste[#,a] (0000-0002-9786-6091).

[a]Laboratory of Biology, Department of Applied Chemistry, Faculty of Chemistry, University of the Basque Country (UPV/EHU), 20018 San Sebastian.

[b]AZTI, Marine Research, Basque Research and Technology Alliance (BRTA), Sukarrieta.

[c]AZTI, Marine Research, Basque Research and Technology Alliance (BRTA), Pasaia.

[d]IKERBASQUE, Basque Foundation for Science, Bilbao

[#] Corresponding author: E-mail: oier.echeveste@ehu.eus; Tel: (+34)943018517; Fax: (+34)943015270; Lab. of Biology, Dept. of Applied Chemistry, Faculty of Chemistry, University of the Basque Country, Manuel de Lardizabal, 3, 20018, San Sebastian.

Keywords. Marine microbes, marine fungi, estuarine fungi, filamentous fungi Sordariomycetes, Hypocreales, CAZYmes, secondary metabolite gene clusters, fucoidan.

Running title. Filamentous fungi from sediments of Basque estuaries

One-sentence summary. Isolation and characterization of filamentous fungi from sediments of Basque estuaries and an assessment of their biotechnological potential.

Importance.

Marine microbes are considered an unlimited source of molecules for biotechnology in fields such as pharmaceutics, biomedicine, cosmetics, nutraceutics, food, feed or agriculture. Thus, it is believed that blue biotechnology will make a significant contribution to the sustainability of global economy. However, the study of marine fungi lags behind that of marine bacteria and it is considered that the potential impact of fungi at the biotechnological level is underestimated. In this work, filamentous fungi from sediment samples of estuaries of the Basque Country have been isolated and the genomes of the Sordariomycete fungi *Marquandomyces marquandii* and *Albophoma yamanashiensis* sequenced and analyzed. Their characterization will contribute to the inventory of the genomic diversity within filamentous fungi and the identification of species and activities with biotechnological potential.

Abstract.

Marine environments harbor a vast diversity of microorganisms, which have developed multiple strategies to adapt to stress conditions such as high salt concentrations and nutrient scarcity and, thus, are a source of natural products and high-value enzymes, as they have the ability to degrade complex polymeric substrates. These features make marine microorganisms a valuable source for the development of new biotechnological tools. Here, we focused on the isolation of filamentous fungi, using sediment samples collected from estuaries of the Basque Country in the Bay of Biscay. The phenotype of these isolates was characterized based on the potential to grow on complex marine polysaccharides or to secrete pigments to the culture medium. Based on this screening, the genomes of two isolates of the order Hypocreales, *Marquandomyces marquandii* and *Albophoma yamanashiensis*, were sequenced and are described here for the first time.

The analysis of their CAZYme (carbohydrate-active enzyme) and secondary metabolite gene-cluster repertoires suggest that these estuarine isolates could be used as a source of novel enzymatic activities and secondary metabolites.

Introduction.

Fungi probably represent the largest and most diverse eukaryotic kingdom (1, 2), with an estimated number of species ranging from 2 to 4 million. Fungi have adapted to very diverse environments and niches (3), including high salt concentrations, nutrient limitation, or environments where the main source of carbon and nitrogen is in form of recalcitrant polymers. The first records of marine fungi have more than a century (4) and the research interest on marine mycology has grown considerably in the last years. However, the state-of-the-art in this field lags behind that of marine bacteria. As a reference, the number of total marine fungal species listed in the Marine Fungi website (https://www.marinefungi.org/; (5)) is 1,857, as of July 2022. In contrast, the bacterial database BacDive (6) includes a subset of 7,916 strains with the tag "*aquatic*", 2,040 strains with the tag "*marine*" and 1,550 strains with the tag "*sediment*" (accessed in July 2023). These numbers would significantly increase if results from culture-independent metabarcoding analyses were considered (7).

It is hypothesized that the number of marine fungal species and their diversity is far larger than presently known. Marine fungal species already deposited in culture collections account for approximately 10 % of the total number of fungal species present in marine environments (4, 8). One of the biggest problems for the advance in this research field is the difficulty for cultivating slow-growing marine fungi under laboratory conditions (9). Overall, it can be concluded that the potential impact of fungi at environmental and biotechnological levels is underestimated (4, 10).

Genome sequencing of some of the cultivable marine fungal strains has revealed biotechnological potential in several fields, such as the identification of new antimicrobials, compounds with antitumoral activity and other secondary metabolites, as well as in bioremediation and wastewater treatment (see references within (11)). Fungal marine strains capable of degrading polysaccharides of marine origin have also been identified (11–13), which are interesting at the biotechnological level. On the one hand, marine polysaccharides include linkages that are difficult to break and thus require specific enzymatic activities. On the other hand, these polysaccharides and the oligosaccharides generated after their partial degradation have shown immunomodulatory, anti-inflammatory, virucidal or anti-cancer activities (14–18).

In this work, sediment samples collected in five estuaries of the Basque Country (Bay of Biscay) were processed in an attempt to isolate filamentous fungi. Within our library of isolates, mainly formed by Sordariomycetes and Eurotiomycetes fungi, we focused our analysis on isolates M60 (*Marquandomyces marquandii*) and M98 (*Albophoma yamanshiensis*), based on their phenotype on culture medium supplemented with polysaccharides of marine origin or their ability to produce and secrete pigments. Genome analysis of both isolates (to our knowledge, the first reported in the literature for these species) included the analysis of their carbohydrate-active enzymes (CAZYmes) and secondary metabolite gene-cluster repertoires. Our results could be used as a source of novel enzymatic activities and secondary metabolites.

Results.

Sordariomycetes, Dothideomycetes and Eurotiomycetes dominate cultivable fungi in coastal marine sediments of the Basque Country

A total of 273 isolates were obtained from coastal sediment samples (including 6 estuarine stations and 1 coastal marine station; see the procedure in Materials and Methods), while 21 additional isolates were obtained from a *F. spiralis* sample (Figure 1A). Figure 1B shows the phenotypic diversity of some of the isolates of our collection when they were cultured on the culture medium used for their isolation. The phenotypes of 235 isolates (80.0 % of the library) were characterized in four of the culture media used for isolation (PDA, MEA, Pc and Lc; Figure S1). The aim was to identify isolates showing the same or similar phenotypes. Our results suggest that multiple isolates correspond to the same strains, or strains of the same species showing subtle phenotypic differences (colored squares in Figure S1).

Genomic DNA of a number of isolates (50; 17.0 % of the library) was extracted. The ITS (internal transcribed spacer) region and/or an internal region of the gene *rpb1* were amplified by PCR from each DNA sample and sequenced (Figure 1C and 1D). Results suggest that Sordariomycetes (genus *Marquandomyces*), Dothideomycetes (genus *Cladosporium*) and Eurotiomycetes (genus *Penicillium*) were the most represented classes and genera in the cultivable mycobiota of estuarine sediments of the Basque Country.

Potential pigment producers.

After a preliminary characterization of the isolates, we initially directed our search towards the identification of producers of pigments (see examples in Figure 2A). Among pigment producers, isolate M60 (estuary of river Artibai, winter 2021) developed purple colonies and stained MEA and mainly PDA media in yellow (Figure 2A-2B), indicating the secretion of pigment(s). Sanger sequencing of the ITS region suggested that isolate M60 was affiliated with *Marquandomyces marquandii*, with a nucleotide identity above

99.4 % when compared with the best hits GU566261.1 and OM647857.1) (19). To our knowledge, there are no previous genomes deposited for this species and, thus, isolate M60 was selected for genome sequencing.

Our microscopic analyses showed that M60 generated hyphal and developmental structures similar to those described for *M. marquandii* (Figure 2B) (19, 20). In liquid minimal medium and after 6 days of culture at 30 ºC and 180 rpm, we did not observe the formation of fully developed conidiophores but formation of side-branches in hyphae, each developing a single conidium (20). The formation of these simplified asexual structures could be a consequence of carbon starvation, as occurs in the model fungus *Aspergillus nidulans* (21, 22).

Phenotypic characterization of isolated fungi on culture medium supplemented with algal polysaccharides.

Three types of fucoidan were used in the phenotypic screening, since the monosaccharide content, linkage type, degree of sulfation and the position of sulfate groups vary significantly among them (23–26). Initially, we found that most isolates were able to grow with fucoidan from *L. japonica* (Figure S2), but this result may be biased due to the fact that the purity of this polysaccharide is not detailed on the website of the supplier. In the case of fucoidan from *F. vesiculosus* or *U. pinnatifida*, which guaranteed a purity above 95 %, differences were found in the growth patterns of the isolates. In general, *the radii* of colonies were higher when fucoidan from *U. pinnatifida* was used compared to that of *F. vesiculosus* (Figure S3), and in both cases, radial growth was significantly restricted compared to the use of fucoidan from *L. japonica*.

Isolate M98, isolated from the estuary of Artibai river in winter 2021, showed a slightly bigger radial growth in minimal medium supplemented with fucoidan of *F. vesiculosus*

than in the negative control, both when ammonium tartrate and sodium nitrate were used as the nitrogen source (Figure 3A). The same phenotype was observed in isolate M127, isolated from a sample of Oria river collected in summer 2021 (Figure 3A). M98 showed a characteristic phenotype, producing pycnidia when cultured on PDA or MEA culture media (Figure 3B) (27). These phenotypic traits had been previously described by Kobayashi and colleagues for *A. yamanashiensis* (28). Thus, isolate M98 was initially associated to this hypocrealean fungus. Sanger sequencing of the ITS region of isolate M98 suggested that this isolate was affiliated with the genus *Tolypocladium* (nucleotide identity above 99.8 % in all cases; accession number of the best hit: AB457003.1) or the species *Albophoma yamanashiensis* (nucleotide identity above 99.6 % in all cases; accession number of the best hit: OW983802.1). Sequencing of *rpb1* suggested that it was affiliated with the genus *Tolypocladium* (nucleotide identity above 96.1 %; accession number of the best hit: KF747240.1). Due to its characteristic phenotype, including the capability of growing on medium supplemented with fucoidan, M98 was selected for genome sequencing.

Genome sequencing and features of isolates M60 and M98.

The size of the assemblies of isolates M60 and M98 was 43.69 Mb and 31.29 Mb, respectively (see general data in Table 1). The number of *contigs* longer than 1,500 bp were 111 and 44 for the two isolates (98 and 41 *contigs*, respectively, longer than 3000 bp). The largest *contigs* of M60 and M98 assemblies were of 5,622,403 and 4,468,825 bp, respectively. Annotation of each assembly led to the prediction of 12,946 and 10,696 proteins for isolates M60 and M98, respectively (Table 1). Completeness estimates were of 97.1 for both assemblies and single-copy BUSCO shares ranged between 96.1 and 96.3 %, indicating high completeness and low redundancy of processed genomic data based on universal single-copy orthologs of Hypocreales (M60 and M98).

Average nucleotide identity (ANI) values were calculated among isolates and different species of the order Hypocreales (Figure 4). The highest ANI value for isolate M98 was obtained, as expected, with *A. yamanshiensis* (99 %) (Figure 4A). Both genomes were phylogenetically related, appearing in the same clade (Figure 4B), next to the main clade of the genus *Tolypocladium* (ANI values between 83 and 92 %).

Isolate M60 was also placed in a clade next to those of the genera *Metarhizium* and *Pochonia* (Figure 4; ANI values of 80 %), which is in agreement with the results described by (19). AAI (average amino acid sequence identity) analyses supported the above-mentioned predictions (not shown).

CAZYme repertoires of *M. marquandii* M60 and *A. yamanashiensis* M98.

There is no public genome sequence of *M. marquandii* (isolate M60), and the genome of *A. yamanashiensis* (99 % ANI with isolate M98) is publicly available (GenBank GCA_001600555.1) but it has not been described in detail. Here, we carried out a characterization of the predicted CAZYme (carbohydrate-active enzymes) and secondary metabolite gene cluster repertoires of both isolates.

A total of 593 and 355 CAZYmes were predicted for M60 and M98, respectively, by at least two of the tools used by dbCAN3 (Figure 5A; Tables S1 and S2). A total of 200 (33.7 %; M60) and 125 (35.2 %; M98) were predicted to include a signal peptide in their sequence and would therefore represent the set of potentially secreted CAZYmes of those isolates. In the case of isolate M60, 95 of the predicted CAZYmes were listed as AA (auxiliary activity family protein), 27 as CBM (carbohydrate-binding module), 22 as CE (carbohydrate esterase), 323 as GH (glycoside hydrolase), 118 as GT (glycosyl transferase) and 8 as PL (polysaccharide lyase). For M98, dbCAN3 predicted a

189 significantly lower number of GHs, 167, together with 51 AAs, 10 CBMs, 13 CEs and
190 114 GTs (no PLs were predicted).

191 Focusing on the CAZYmes and sulfatases potentially involved in the degradation of
192 fucoidan, several relevant protein families were found, such as GH29 (2 and 1 in M60
193 and M98, respectively), GH95 (6 and 1), GH141 (1 and 0), GH36 (8 and 1) and GH28 (7
194 and 1). In addition, glycosyl hydrolase families potentially involved in the degradation of
195 ulvan, another sulfated algal polysaccharide, were identified, such as GH2 (16 and 4),
196 GH3 (17 and 8), GH39 (4 and 0), GH43 (9 and 0), GH78 (2 and 0), GH88 (4 and 0) and
197 GH105 (4 and 1). Predictions by dbCAN3 agreed with the prediction of the three-
198 dimensional fold of the corresponding families with ColabFold (see specific examples in
199 Figure 5B).

200 SulfAtlas predicted that the genomes of fungal isolates M60 and M98 included a few
201 sulfatases of families S1_4 (4 and 0, respectively), S1_6 (2 and 2), S1_8 (2 and 0), S1_11
202 (0 and 1) S1_12 (1 and 1), S2 (2 and 1) and S3 (3 and 2, in M60 and M98, respectively).
203 Overall, the repertoire of predicted fucoidan-degrading enzymes in the fungal isolates
204 characterized here is far more limited than the one described in the literature for fucoidan-
205 degrading marine bacteria (26) (see Discussion).

206 **Secondary metabolite gene cluster analyses.**

207 The fungal version of antiSMASH was used to assess the potential of isolates M60 and
208 M98 to produce secondary metabolites (29). Figure 6 summarizes the number of genes
209 coding for backbone enzymes found by antiSMASH in the genomes of *M. marquandii*
210 (M60) and *A. yamanashiensis* (M98) isolates (see also Figures S4-S5).

AntiSMASH predicted the presence of 77 secondary metabolite gene clusters in the genome of isolate M60 (Figure 7). It includes 10 secondary metabolite gene clusters (Figure 7) with similarity percentages higher than 70 % (similarity, in this case, refers to the percentage of genes within the closest known cluster that have a significant BLAST hit to genes within the predicted cluster) (Figure S4). A similarity percentage of 100 % was assigned to clusters N2-C4 (ε-Poly-L-lysine, a non-ribosomal peptide), N3-C2 (choline; non-ribosomal peptide), N9-C1 (FR901512; polyketide), N12-C1 (metachelin; non-ribosomal peptide), N15-C1 (1,3,5,8-tetrahydroxynaphthalene; polyketide), N16-C1 (dymethylcoprogen, non-ribosomal peptide) and M19-C1 (peramine; non-ribosomal peptide).

In the case of the *A. yamanashiensis* isolate (M98), antiSMASH predicted the presence of 53 secondary metabolite gene clusters (Figure S5), which suggests a more limited potential for secondary metabolite production than in the case of isolate M60 (*M. marquandii*). AntiSMASH identified 6 secondary metabolite gene clusters (Figure 8) with similarity percentages higher than 70 % compared to those known to synthesize the compounds as indicated in Figure S5. A similarity percentage of 100 % was assigned to clusters N1-C8 (metachelins; non-ribosomal peptide), N2-C2 (terpendole E; a terpenic acyl-CoA:cholesterol acyltransferase inhibitor known to be produced by *A. yamanashiensis*) (30), N5-C1 (choline; non-ribosomal peptide) and N7-C3 (tolypyridone C; polyketide + non-ribosomal peptide).

Discussion.

The application of the *dilution-to-extinction* method (9) in estuarine sediment samples enabled the isolation of a large diversity of filamentous fungi showing a variety of growth patterns. Our results by ITS sequencing suggest that cultivable fungi from the estuaries

of study are mainly represented by Eurotiomycetes and Sordariomycetes species. This agrees with previous culture-based studies where marine fungi seemed to be dominated by Eurotiomycetes (*e.g.*, *Aspergillus* and *Penicillium*), Sordariomycetes (*e.g.*, *Fusarium*, *Trichoderma*, *Paecilomyces-Marquandomyces*) and Dothideomycetes (*e.g.*, *Cladosporium* and *Ulocladium*) (see references within (5)). Nevertheless, the extreme differences in growth rates among marine fungal species in culture (9) may be biasing the real composition of fungi in the samples, as typically found for bacteria (*i.e.*, the great plate-count anomaly; (31)). Additional efforts in isolation and culturing of slow-growing fungi and the direct identification of fungal taxa by metabarcoding (see, for example, (32–34)) will contribute to the identification of previously undescribed species, some of them potentially harboring biotechnological potential.

The repertoire of secondary metabolism backbone enzymes in fungi is composed mainly of PKS, NRPS, dimethylallyltransferases (DMATs), and terpene synthases (35), and the number of biosynthetic gene clusters per genome varies dramatically across different species (35, 36). Here, we have focused on the description of specific genomic features of two species that were previously described phenotypically (19, 20, 28) but not at the genomic level. Interestingly, in both cases, the strains characterized phenotypically were originally isolated from terrestrial environments. On the one hand, *M. marquandii* has been reported to grow on mushrooms and soil, and their distribution covered Brazil, Netherlands, Russia, UK and USA (19). On the other hand, *A. yamanshiensis* was isolated from a forest soil in Japan (28). The isolation of strains of both species in sediment samples of Basque estuaries suggests that they are ubiquitously distributed and have adapted also to marine and estuarine environments. While both isolates, M60 and M98, correspond to species of the order of Hypocreales, the number of backbone enzyme-

coding genes and secondary metabolite gene clusters is clearly higher in isolate M60 than in the genome of isolate M98, in correlation with the size of their genomes.

Isolate M60 was selected in this work for genome sequencing as the *M. marquandii* genome (synonims *Metarhizium marquandii* and *Paecilomyces marquandii*) had not been previously deposited and described. This strain was able to produce a yellow pigment, which synthesis and secretion clearly depended on the composition of the culture medium (Figure 2A), as previously shown (19). Using a *M. marquandii* strain isolated from a marine sediment sample collected in Argentina, Cabrera *et al*. described that the yellow pigment is a nitrogen-containing sorbicillinoid (sorbicillinoid urea) and proposed a biosynthetic pathway (37, 38). In general, sorbicillinoids represent an important family of hexaketide compounds produced by terrestrial and marine fungi, including species of *Marquandomyces*/*Paecilomyces*, and have a variety of biological activities including cytotoxic, antioxidant, antiviral and antimicrobial activity (39). Remarkably, we found that isolates closely related to M60, such as M43-45, affiliated with *Marquandomyces marquandii*, showed similar but not identical phenotypes. In the case of isolate M45, we have not observed the production of the characteristic yellow metabolite secreted by M60 (19, 20). Comparative genomic analysis of these strains could contribute to the identification of point substitutions or insertions/deletions causing an inhibition of the synthesis of the mentioned yellow pigment.

We identified a biosynthetic gene cluster in the genome of M60 (N6-C5) which is probably related to sorbicillin biosynthesis, as it shows high identity with the sorbicillin gene cluster of *Penicillium chrysogenum* (Figure S4) (35). The sorbicillin biosynthesis gene cluster described in *P. chrysogenum* includes two PKS-encoding genes, *sorA* and *sorB*, and two transcription factor-coding genes, *sorR1* and *sorR2* (SorR1 acts as an activator, while SorR2 controls the expression of *sorR1*) (40). Sorbicillin clusters have

been described in additional fungal species, such as *T. reesei* (41). Here, cluster N6-C5 included genes encoding the two PKSs (g7028 and g7029) and the two transcription factors (g7023 and g7025) (Figure 7). RNA sequencing experiments comparing samples cultured in PDA versus MEA media would confirm the upregulation of cluster N6-C5 in PDA and would inform of up- or downregulation of the rest of secondary metabolism gene clusters identified in the genome of isolate M60. Considering that, across fungi, the vast majority of gene cluster families are species specific (35), transcriptomic analyses will be important to determine the biosynthetic potential of isolate M60 and the rest of isolates of our library.

In the case of M98, this isolate was selected for genome analysis because the genome of *A. yamanshiensis* had not been described in detail and due to their apparent growth on fucoidan. For the degradation of this marine polysaccharide, several glycosyl hydrolases have been described belonging to families GH29 (α-L-fucosidase), GH95 (α-L-fucosidase/α-L-galactosidase), GH141 (α-L-fucosidase/xylanase) and GH107 (endo-α-L-fucanase) (Sichert et al., 2020). The same authors also described that families GH36 (α-galactosidase, α-N-acetylgalactosaminidase, stachyose synthase, raffinose synthase), GH116 (β-glucosidase, β-xylosidase, acid β-glucosidase/β-glucosylceramidase, β-N-acetylglucosaminidase), and GH117 (β-D-galactofuranosidase, α-neoagaro-oligosaccharide hydrolase) may be fucoidanases with a yet unknown function, and that families GH28 (polygalacturonase) and GH155 (glucuronidase; family removed from the CAZYme database; (42)) remove acetate, galacturonic acid and glucoronic acid, which are present in specific types of fucoidan.

Regarding the analysis of sulfatases, subfamilies S1_15, S1_16, S1_17 and S1_25 have been reported as necessary for fucoidan degradation or enriched in fucoidan-degrading marine bacterial proteomes (26). On the other hand, glycosyl hydrolases and sulfatases

required for the degradation of ulvan, another algal polysaccharide composed of sulfated rhamnose, glucuronic and iduronic acids, and xylose (43), belong to families GH2, GH3, GH39, GH43, GH78, GH88, GH105, S1_7, S1_25 and PL28 (44). Our results show that the predicted repertoire of fucoidan-degrading protein families in *A. yamanashiensis* is more limited than in *M. marquandii*, and the set of sulfatases in these two fungal isolates is completely different compared to fucoidan-degrading bacteria. Interestingly, M60 includes at least one member of families GH29, GH95 and GH141, and all the glycosyl hydrolase families described to be involved in ulvan degradation. It must be considered, however, that dissimilar modes of action have been described within the same subfamily of glycosyl hydrolases (44). In this context, the ability of both isolates to degrade sulfated algal polysaccharides should be analyzed in detail in the future.

Results by Sichert and colleagues support the idea that the complex structures of fucoidans require a large number of enzymes for their degradation (26). It is yet to be determined whether this subset of CAZYmes has expanded in bacteria as a result of functional redundancy, specific functionality on the different types of linkages of fucoidans, or both, but this seems not to be the trend in fungi. Alternatively, degradation of recalcitrant marine polysaccharides such as fucoidan could follow completely different mechanisms in bacteria and fungi, with different subsets of CAZYmes involved. Transcriptomic analyses will be essential to confirm or discard this possibility.

Conclusions.

Cultivable filamentous fungal populations in sediments of the studied sites from Basque estuaries consist of mainly Sordariomycete, Dothideomycetes and Eurotiomycete species, including some species with biotechnological potential. The genomes of our *Marquandomyces marquandii* and *Albophoma yamanashiensis* isolates encode

CAZYmes potentially involved in the degradation of sulfated polysaccharides and include secondary metabolite gene clusters of potential interest, and these activities will have to be confirmed and analyzed in detail in the future.

Materials and Methods.

Sample collection and Processing.

Seven stations along the Basque coast (Bay of Biscay) were selected for sampling (Figure 9) based on organic content and granulometry properties. One of these stations is located offshore, at approximately 0.8 km from the coast, and the depth is 37 m (black square in Figure 9). Samples were collected during winter and spring of 2021, in 50 mL polypropylene tubes, which were stored at 4 ºC until processing. Additionally, samples of the macroalgae *Fucus spiralis* were collected in Hondarribia (Basque Country) for the isolation of their associated fungi.

For isolation of fungi from both sources, the *dilution-to-extinction* method was used (9) based on the procedure developed by Velez and coworkers (45). Briefly, approximately two centimeters of the upper layer of the sediment were removed using a sterile spatula. Samples of 1.4-2.2 g were taken from the center of each tube (material that was not in contact with the wall of the tube) and transferred to 15 mL polypropylene tubes. Sediment samples were diluted serially (1/5 once and 1/10 twice) in artificial seawater (see below). In the case of the *Fucus spiralis* samples, the macroalgae were washed with artificial sea water and samples were collected from the surface and diluted serially in a similar procedure. Aliquots of 50 µL per well were inoculated in 24-well plates previously filled with the culture medium (see below) plus penicillin. One well per plate was inoculated with artificial sea water as a control for potential contaminations. Plates were covered with aluminum paper and cultured under aerobic conditions at atmospheric pressure and

357 25 ºC. Growth of microorganisms was checked regularly and samples of isolates
358 generating filaments were transferred to plates containing the same culture medium used
359 for isolation, until homogeneous phenotypes, and thus probably axenic cultures, were
360 obtained. Specific isolates showed an invasive behavior, colonizing adjacent wells in
361 multi-well plates. To minimize the risk of contamination, the latter isolates were
362 discarded from the analysis. Samples of all selected isolates were stored at -80 ºC in a
363 glycerol solution (18% in artificial sea water).

364 **Preparation of culture media and solutions.**

365 Artificial sea water solutions were prepared by diluting 90 g of sea salts purchased from
366 Sigma-Aldrich per liter of distilled water (3x stock; 9%) (12). Alternatively, a 4x stock,
367 sterilized by vacuum filtration (pore diameter: 0.45 µm), was prepared by adding 46.94 g
368 NaCl, 7.84 g Na_2SO_4, 21.28 g $MgCl_2.6H_2O$, 2.2 g $CaCl_2$, 0.384 g $NaHCO_3$, 1.328 g KCl,
369 0.192 g KBr, 0.052 g H_3BO_3, 0.048 g $SrCl_2$ and 0.006 g NaF per liter of distilled water
370 (46). Penicillin sodium salt was added to all culture media (0.018 mg/mL; 30 units/mL).

371 Six types of media were used for isolation of filamentous microbes from estuarine
372 sediments. In a first screen, the following culture media (1/5 dilution of the standard; 15
373 g of agar per liter) were used: 1) malt extract agar (MEA; Condalab; 2.69 g of the powder,
374 133 mL of the 3x sterile artificial sea water solution and distilled water to 400 mL); 2)
375 potato dextrose agar (PDA; Condalab; 3.12 g of the powder, 133 mL of the 3x sterile
376 artificial sea water solution and distilled water to 400 mL); 3) corn meal agar (CMA;
377 Condalab; 1.36 g of the powder, 133 mL of the 3x sterile artificial sea water solution and
378 distilled water to 400 mL); 4) Lc medium (2g Arabic gum, 2 g olive oil, 0.2 g yeast extract,
379 0.4 g peptone, 2.42 g PIPES (1,4-Piperazinediethanesulfonic acid), 133 mL of the 3x
380 sterile artificial sea water solution and distilled water to 400 mL; pH adjusted to 7.5 with

NaOH); and 5) Pc medium (3.6 g brain heart infusion, 9.2 g NaCl, 2.42 g PIPES, 133 mL of the 3x sterile artificial sea water solution and distilled water to 400 mL; pH adjusted to 7.5 with NaOH) (45, 47, 48).

A minimal medium supplemented with different carbon and nitrogen sources was also prepared by adding, per liter, 250 mL of the 4x stock of artificial sea salt solution and 10 mL of a salts plus trace elements solution (25 mL of a trace elements solution, 50 g KH_2PO_4, 10 g $MgSO_4.7H_2O$, 5 g $CaCl_2.2H_2O$ per liter) (12). The trace elements solution (40x) was prepared by adding, per liter, 20 g monohydrated citric acid, 20 g $ZnSO_4.7H_2O$, 2.84 g $FeSO_4.7H_2O$, 0.15 g $MnSO_4.H_2O$, 1.04 g $CuSO_4.5H_2O$, 0.2 g H_3BO_3, 0.15 g $(NH_4)_6Mo_7O_{24}.4H_2O$ and 0.2 g biotin.

To ease the screening of isolates with biotechnological potential, we decided to use solid minimal medium. First, agar concentration had to be decreased as low as possible because it could be used by the isolates as a carbon source. Agar concentration was decreased from 1.5 % (45) to 0.4-0.5 %, which was the minimum agar concentration allowing solidification of the culture medium and clean point inoculation (Figure S6). Minimal medium (0.5 % agar) without the addition of an extra carbon source was used as a negative control, while the addition of glucose (2 g/L) was used as a positive control of growth. The polysaccharides alginate (Sigma-Aldrich) or fucoidan (*Laminaria japonica*, Carbosynth; *Fucus vesiculosus*, Sigma-Aldrich; or *Undaria pinnatifida*, Sigma-Aldrich) were added at a concentration of 2 g/L (20 g/L stocks). The phenotypes in these culture media were compared to those shown in minimal medium with the polysaccharide laminarin (from *Thallus laminariae*; Carbosynth; also, at 2 g/L), which in general is more easily degraded by microorganisms (11). Ammonium tartrate (positive balance of protons; 9.2 g/100mL; 100x) or sodium nitrate (negative balance of protons; 4.25 g/100mL; 100x) were added as the main nitrogen sources, to compare any possible effect

406 of the proton balance in the growth of fungal isolates, and also a hypothetic use of tartrate
407 as a carbon source. Overall, we considered an isolate for further analysis when it showed
408 greater radial growth rate on minimal medium supplemented with the polysaccharide than
409 on minimal medium without an extra carbon source (negative control; only
410 bacteriological agar). This phenotype had to be observed both when ammonium tartrate
411 or sodium nitrate was used as the nitrogen source.

412 **Microscopic analysis of fungal growth and development.**

413 Isolates were inoculated in liquid minimal medium supplemented with glucose and
414 ammonium tartrate and cultured at 180 rpm and 30 ºC. Culture times varied depending
415 on the growth rate of each isolate. Samples of each culture were analyzed using a Nikon
416 Eclipse E100 microscope equipped with an Imaging Source DFK23UP031 camera.
417 Alternatively, a Nikon Eclipse Ci manual upright microscope was used, which included
418 40× and 100× (oil) Nikon CFI Plan Fluor lenses and a Teledyne Photometrics Moment
419 camera. ImageJ (https://imagej.nih.gov/ij/) (US. National Institutes of Health, Bethesda,
420 MA, USA) was used to process phase contrast images.

421 **Extraction of genomic DNA, ITS amplification and Sanger sequencing.**

422 Isolates were cultured in liquid minimal medium (28 ºC, 170 rpm) supplemented with
423 ammonium tartrate and glucose as nitrogen and carbon sources. Incubation times varied
424 depending on the growth rate of each isolate. Mycelia were filtered using Miracloth paper
425 and lyophilized. Samples were processed with a Next Advance Bullet Blender
426 homogenizer and genomic DNA fractions were extracted following the 1)
427 phenol:chloroform:isoamylalcohol (25:24:1; Panreac AppliChem) method or 2) the
428 guidelines of the NucleoSpin Plant II Mini kit (Macherey-Nagel). The integrity of the
429 samples was checked by agarose electrophoresis (0.8 %).

430 Using genomic DNA samples as template, ITS regions or a fragment of the gen *rpb1*,
431 which encodes the main subunit of the RNA polymerase II complex, were amplified using
432 oligonucleotide pairs ITS5 (GGAAGTAAAAGTCGTAACAAGG) and ITS4
433 (TCCTCCGCTTATTGATATGC), ITS4 and ITS1 (TCCGTAGGTGAACCTGCGG),
434 and/or Rpb1-Up (GAATGCCCAGGTCATTTCGG) and Rpb1-Dw
435 (CCAGCGATATCGTTGTCCATATA) (45, 49, 50). The Kapa Taq DNA polymerase
436 (Kapa Biosystems) was used for amplification (denaturation: 30 seconds at 95 ºC;
437 annealing: 30 seconds at 54 ºC; elongation: 60 seconds at 72 ºC; 25 cycles). Amplification
438 and specificity of the amplicons were checked by agarose electrophoresis (2 %).
439 Amplicons were purified using the Macherey-Nagel NucleoSpin gel and PCR clean-up
440 kit and Sanger sequenced at Secugen S.L. (Madrid, Spain).

441 **Genome sequencing.**

442 Genomes of isolates M60 and M98 were initially sequenced using the Illumina MiSeq
443 platform at the General Services of the University of the Basque Country (UPV/EHU),
444 and later re-sequenced at the CNAG (https://www.cnag.crg.eu/) by combining the
445 Illumina NovaSeq platform and nanopore (GridION) sequencing. Samples were quality-
446 checked at the UPV/EHU and CNAG facilities before sequencing. The two whole
447 genome shotgun projects were deposited in the GenBank database under accession
448 numbers JAUIRS000000000 for isolate M60 (BioProject PRJNA990752; BioSample
449 SAMN36274215), and JAUIRT000000000 for isolate M98 (BioProject PRJNA990765;
450 BioSample SAMN36274349).

451 **Bioinformatic analyses.**

452 The platform Galaxy (v22.05.1) was used to process genome-sequencing data (51). The
453 workflow *Itsas_Genomak* can be accessed in the following link:

454 https://usegalaxy.org/u/oilier/h/itsasgenomak. Spades (versions v3.13.1) was used to
455 assemble genomes from all Illumina and nanopore sequencing files (52). Augustus
456 (v3.4.0) (53) was used for gene annotation. BUSCO (Benchmarking Universal Single-
457 Copy Orthologs; v5.2.2) was used for the assessment of the completeness of genome
458 assemblies (54, 55). BLASTs and HMM analyses were carried out at NCBI (56) and
459 Sulfatlas websites (v2.3.1) (57). ANI (average nucleotide identity) and AAI (average
460 amino acid identity) for species proximity were carried out at enveomics (58) and with
461 AAI-profiler (59) (both websites were accessed in September 2022, and May 2023). The
462 genomes and proteomes used in ANI and AAI analyses were downloaded from the NCBI
463 database (Table S3). CAZYme analyses were carried out at the dbCAN website (accessed
464 in May 2022, and June 2023; (60, 61)). The dbCAN website uses three tools for
465 automated CAZYme annotation: HMMER for annotated CAZYme domain boundaries,
466 DIAMOND for fast blast hits in the CAZY database and HMMER for dbCAN-sub, a
467 database of carbohydrate active enzyme subfamilies for substrate annotation. Following
468 the recommendation of the website, we excluded from our analyses all the CAZYmes
469 predicted only by one of those three tools (431 and 305 in the case of M60 and M98,
470 respectively). AntiSMASH 6.0 and 7.0 were used for the identification of secondary
471 metabolite gene clusters (29, 62). ColabFold was used to predict the three-dimensional
472 structure of proteins (63).

473 **Acknowledgements.**

474 We want to thank all groups and members of the EMOTION consortium, funded by the
475 Basque Government (see Funding), for their support. The authors would like to thank the
476 General Research Services of the UPV/EHU (SGIker) and the CNAG-CRG for assistance
477 with genome sequencing projects.

Work at UPV/EHU and AZTI labs was funded by the Basque Government, projects KK-2021/00034 and KK-2022/00107. UPV/EHU lab also thanks the University of the Basque Country for grant GIU19/04 and the Basque Government for grants IT1662-22 and PIBA_2020_1_0032_GVB0. The funders had no role in study design, data collection and interpretation, or the decision to submit the work for publication.

O.E. and L.A.-S. conceived the project. A.O., Z.A., C.P.-C, R.L., A.L. and O.E. performed the experiments. All authors analyzed the results. O.E. and A.O. wrote the first version of the manuscript. All authors reviewed and improved the manuscript.

Conflict of interest.

The authors declare no conflict of interest.

References.

1. Spatafora JW, Aime MC, Grigoriev I V., Martin F, Stajich JE, Blackwell M. 2017. The fungal tree of life: from molecular systematics to genome-scale phylogenies. Microbiol Spectr 5.

2. Stajich JE. 2017. Fungal genomes and insights into the evolution of the kingdom. Microbiol Spectr 5.

3. Hawksworth DL, Lücking R. 2017. Fungal diversity revisited: 2.2 to 3.8 million species. Microbiol Spectr 5.

4. Amend A, Burgaud G, Cunliffe M, Edgcomb VP, Ettinger CL, Gutiérrez MH, Heitman J, Hom EFY, Ianiri G, Jones AC, Kagami M, Picard KT, Quandt CA, Raghukumar S, Riquelme M, Stajich J, Vargas-Muñiz J, Walker AK, Yarden O, Gladfelter AS. 2019. Fungi in the marine environment: open questions and unsolved problems. MBio 10:e01189-18.

5. Jones EBG, Pang K-L, Abdel-Wahab MA, Scholz B, Hyde KD, Boekhout T, Ebel R, Rateb ME, Henderson L, Sakayaroj J, Suetrong S, Dayarathne MC, Kumar V, Raghukumar S, Sridhar KR, Bahkali AHA, Gleason FH, Norphanphoun C. 2019. An online resource for marine fungi. Fungal Divers 96:347–433.

6. Reimer LC, Sardà Carbasse J, Koblitz J, Ebeling C, Podstawka A, Overmann J. 2022. BacDive in 2022: the knowledge base for standardized bacterial and archaeal data. Nucleic Acids Res 50:D741–D746.

7. Klemetsen T, Raknes IA, Fu J, Agafonov A, Balasundaram S V, Tartari G, Robertsen E, Willassen NP. 2018. The MAR databases: development and implementation of databases specific for marine metagenomics. Nucleic Acids Res 46:D692–D699.

8. Jones EBG, Suetrong S, Sakayaroj J, Bahkali AH, Abdel-Wahab MA, Boekhout T, Pang K-L. 2015. Classification of marine Ascomycota, Basidiomycota, Blastocladiomycota and Chytridiomycota. Fungal Divers 73:1–72.

9. Overy DP, Rämä T, Oosterhuis R, Walker AK, Pang K-L. 2019. The neglected marine fungi, *sensu stricto*, and their isolation for natural products' discovery. Mar Drugs https://doi.org/10.3390/md17010042.

10. Kramer A, Labes A. 2020. 16 Biotechnology of Marine Fungi: New Workhorses and Applications BT - Genetics and Biotechnology, p. 399–412. *In* Benz, JP, Schipper, K (eds.), . Springer International Publishing, Cham.

11. Balabanova L, Slepchenko L, Son O, Tekutyeva L. 2018. Biotechnology potential of marine fungi degrading plant and algae polymeric substrates. Front Microbiol 9:1527.

12. Wang Y, Barth D, Tamminen A, Wiebe MG. 2016. Growth of marine fungi on polymeric substrates. BMC Biotechnol 16:3.

13. Kumar A, Sørensen JL, Hansen FT, Arvas M, Syed MF, Hassan L, Benz JP, Record E, Henrissat B, Pöggeler S, Kempken F. 2018. Genome sequencing and analyses of two marine fungi from the North Sea unraveled a plethora of novel biosynthetic gene clusters. Sci Rep 8:10187.

14. Kwon PS, Oh H, Kwon S-J, Jin W, Zhang F, Fraser K, Hong JJ, Linhardt RJ, Dordick JS. 2020. Sulfated polysaccharides effectively inhibit SARS-CoV-2 in vitro. Cell Discov 6:50.

15. Yim S-K, Kim K, Kim I, Chun S, Oh T, Kim J-U, Kim J, Jung W, Moon H, Ku B, Jung K. 2021. Inhibition of SARS-CoV-2 virus entry by the crude polysaccharides of seaweeds and Abalone Viscera *In Vitro*. Mar Drugs https://doi.org/10.3390/md19040219.

16. Feng Y, Wassie T, Gan R, Wu X. 2022. Structural characteristics and immunomodulatory effects of sulfated polysaccharides derived from marine algae. Crit Rev Food Sci Nutr 1–17.

17. Yao W, Qiu H-M, Cheong K-L, Zhong S. 2022. Advances in anti-cancer effects and underlying mechanisms of marine algae polysaccharides. Int J Biol Macromol 221:472–485.

18. Wang M, Veeraperumal S, Zhong S, Cheong K-L. 2023. Fucoidan-derived functional oligosaccharides: Recent developments, preparation, and potential applications. Foods https://doi.org/10.3390/foods12040878.

19. Mongkolsamrit S, Khonsanit A, Thanakitpipattana D, Tasanathai K, Noisripoom W, Lamlertthon S, Himaman W, Houbraken J, Samson RA, Luangsa-ard J. 2020. Revisiting *Metarhizium* and the description of new species from Thailand. Stud Mycol 95:171–251.

20. Samson RA. 1974. *Paecilomyces* and some allied Hyphomycetes. Stud Mycol 6:1–119.

21. Skromne I, Sanchez O, Aguirre J. 1995. Starvation stress modulates the expression of the *Aspergillus nidulans brlA* regulatory gene. Microbiology 141:21–28.

22. Etxebeste O, Markina-Iãrrairaegui A, Garzia A, Herrero-García E, Ugalde U, Espeso EA. 2009. Kapl, a non-essential member of the Pse1p/Imp5 karyopherin family, controls colonial and asexual development in *Aspergillus nidulans*. Microbiology 155:3934–3945.

23. Ale MT, Mikkelsen JD, Meyer AS. 2011. Important determinants for fucoidan bioactivity: A critical review of structure-function relations and extraction methods for fucose-containing sulfated polysaccharides from brown seaweeds. Mar Drugs https://doi.org/10.3390/md9102106.

24. Zhao Y, Zheng Y, Wang J, Ma S, Yu Y, White WL, Yang S, Yang F, Lu J. 2018. Fucoidan extracted from *Undaria pinnatifida*: Source for nutraceuticals/functional foods. Mar Drugs https://doi.org/10.3390/md16090321.

25. Koh HSA, Lu J, Zhou W. 2019. Structure characterization and antioxidant activity of fucoidan isolated from *Undaria pinnatifida* grown in New Zealand. Carbohydr Polym 212:178–185.

26. Sichert A, Corzett CH, Schechter MS, Unfried F, Markert S, Becher D, Fernandez-Guerra A, Liebeke M, Schweder T, Polz MF, Hehemann J-H. 2020. Verrucomicrobia use hundreds of enzymes to digest the algal polysaccharide fucoidan. Nat Microbiol 5:1026–1039.

27. Uchida R, Imasato R, Yamaguchi Y, Masuma R, Shiomi K, Tomoda H, Ōmura S. 2005. New Sesquicillins, insecticidal antibiotics produced by *Albophoma sp.* FKI-1778. J Antibiot (Tokyo) 58:397–404.

28. Kobayashi T, Masuma R, Omura S, Watanabe K. 1994. Materials for the fungus flora of Japan (47). Mycoscience 35:399–401.

29. Blin K, Shaw S, Kloosterman AM, Charlop-Powers Z, van Wezel GP, Medema MH, Weber T. 2021. antiSMASH 6.0: improving cluster detection and comparison capabilities. Nucleic Acids Res 49:W29–W35.

30. Huang X, Tomoda H, Nishida H, Masuma R, Omura S. 1995. Terpendoles, novel ACAT inhibitors produced by *Albophoma yamanashiensis*. I. Production, isolation and biological properties. J Antibiot (Tokyo) 48:1–4.

31. Staley JT, Konopka A. 1985. Measurement of *in situ* activities of nonphotosynthetic microorganisms in aquatic and terrestrial habitats. Annu Rev Microbiol 39:321–346.

32. Banos S, Gysi DM, Richter-Heitmann T, Glöckner FO, Boersma M, Wiltshire KH, Gerdts G, Wichels A, Reich M. 2020. Seasonal dynamics of pelagic mycoplanktonic communities: Interplay of taxon abundance, temporal occurrence, and biotic interactions. Front Microbiol 11:1305.

33. da Silva MK, de Souza LMD, Vieira R, Neto AA, Lopes FAC, de Oliveira FS, Convey P, Carvalho-Silva M, Duarte AWF, Câmara PEAS, Rosa LH. 2022. Fungal and fungal-like diversity in marine sediments from the maritime Antarctic assessed using DNA metabarcoding. Sci Rep 12:21044.

34. Ogaki MB, Pinto OHB, Vieira R, Neto AA, Convey P, Carvalho-Silva M, Rosa CA, Câmara PEAS, Rosa LH. 2021. Fungi present in Antarctic deep-sea sediments assessed using DNA Metabarcoding. Microb Ecol 82:157–164.

35. Robey MT, Caesar LK, Drott MT, Keller NP, Kelleher NL. 2021. An interpreted atlas of biosynthetic gene clusters from 1,000 fungal genomes. Proc Natl Acad Sci 118:e2020230118.

36. Khaldi N, Seifuddin FT, Turner G, Haft D, Nierman WC, Wolfe KH, Fedorova ND. 2010. SMURF: Genomic mapping of fungal secondary metabolite clusters. Fungal Genet Biol 47:736–741.

37. Cabrera GM, Butler M, Rodriguez MA, Godeas A, Haddad R, Eberlin MN. 2006. A Sorbicillinoid Urea from an intertidal *Paecilomyces marquandii*. J Nat Prod

69:1806–1808.

38. Harned AM, Volp KA. 2011. The sorbicillinoid family of natural products: Isolation, biosynthesis, and synthetic studies. Nat Prod Rep 28:1790–1810.

39. Meng J, Wang X, Xu D, Fu X, Zhang X, Lai D, Zhou L, Zhang G. 2016. Sorbicillinoids from fungi and their bioactivities. Molecules https://doi.org/10.3390/molecules21060715.

40. Guzmán-Chávez F, Salo O, Nygård Y, Lankhorst PP, Bovenberg RAL, Driessen AJM. 2017. Mechanism and regulation of sorbicillin biosynthesis by *Penicillium chrysogenum*. Microb Biotechnol 10:958–968.

41. Derntl C, Guzmán-Chávez F, Mello-de-Sousa TM, Busse H-J, Driessen AJM, Mach RL, Mach-Aigner AR. 2017. *In vivo* study of the sorbicillinoid gene cluster in *Trichoderma reesei*. Front Microbiol 8.

42. Cartmell A, Muñoz-Muñoz J, Briggs JA, Ndeh DA, Lowe EC, Baslé A, Terrapon N, Stott K, Heunis T, Gray J, Yu L, Dupree P, Fernandes PZ, Shah S, Williams SJ, Labourel A, Trost M, Henrissat B, Gilbert HJ. 2019. Author Correction: A surface endogalactanase in *Bacteroides thetaiotaomicron* confers keystone status for arabinogalactan degradation. Nat Microbiol 4:2021–2023.

43. Kidgell JT, Magnusson M, de Nys R, Glasson CRK. 2019. Ulvan: A systematic review of extraction, composition and function. Algal Res 39:101422.

44. Reisky L, Préchoux A, Zühlke M-K, Bäumgen M, Robb CS, Gerlach N, Roret T, Stanetty C, Larocque R, Michel G, Song T, Markert S, Unfried F, Mihovilovic MD, Trautwein-Schult A, Becher D, Schweder T, Bornscheuer UT, Hehemann J-H. 2019. A marine bacterial enzymatic cascade degrades the algal polysaccharide ulvan. Nat Chem Biol 15:803–812.

45. Velez P, Gasca-Pineda J, Riquelme M. 2020. Cultivable fungi from deep-sea oil reserves in the Gulf of Mexico: Genetic signatures in response to hydrocarbons. Mar Environ Res 153:104816.

46. Wiegand S, Jogler M, Boedeker C, Pinto D, Vollmers J, Rivas-Marín E, Kohn T, Peeters SH, Heuer A, Rast P, Oberbeckmann S, Bunk B, Jeske O, Meyerdierks A, Storesund JE, Kallscheuer N, Lücker S, Lage OM, Pohl T, Merkel BJ, Hornburger P, Müller R-W, Brümmer F, Labrenz M, Spormann AM, Op den Camp HJM, Overmann J, Amann R, Jetten MSM, Mascher T, Medema MH, Devos DP, Kaster A-K, Øvreås L, Rohde M, Galperin MY, Jogler C. 2020. Cultivation and functional characterization of 79 planctomycetes uncovers their unique biology. Nat Microbiol 5:126–140.

47. Burgaud G, Le Calvez T, Arzur D, Vandenkoornhuyse P, Barbier G. 2009. Diversity of culturable marine filamentous fungi from deep-sea hydrothermal vents. Environ Microbiol 11:1588–1600.

48. Thomas LC, Gaëtan B, Stéphane M, Georges B, Philippe V. 2009. Fungal diversity in deep-sea hydrothermal ecosystems. Appl Environ Microbiol 75:6415–6421.

49. White TJ. 1990. Amplification and direct sequencing of fungal ribosomal RNA genes for phylogenetics, p. 315–322. *In* Innis, MA, Gelfand, DH, Sninsky, JJ, White, TJ (eds.), PCR Protocols: A Guide to Methods and Applications. Academic Press.

50. Toju H, Tanabe AS, Yamamoto S, Sato H. 2012. High-coverage ITS primers for the DNA-based identification of Ascomycetes and Basidiomycetes in environmental samples. PLoS One 7:e40863.

51. Afgan E, Baker D, Batut B, van den Beek M, Bouvier D, Čech M, Chilton J, Clements D, Coraor N, Grüning BA, Guerler A, Hillman-Jackson J, Hiltemann S, Jalili V, Rasche H, Soranzo N, Goecks J, Taylor J, Nekrutenko A, Blankenberg D. 2018. The Galaxy platform for accessible, reproducible and collaborative biomedical analyses: 2018 update. Nucleic Acids Res 46:W537–W544.

52. Bankevich A, Nurk S, Antipov D, Gurevich AA, Dvorkin M, Kulikov AS, Lesin VM, Nikolenko SI, Pham S, Prjibelski AD, Pyshkin A V, Sirotkin A V, Vyahhi N, Tesler G, Alekseyev MA, Pevzner PA. 2012. SPAdes: A new genome assembly algorithm and its applications to single-cell sequencing. J Comput Biol 19:455–477.

53. Stanke M, Keller O, Gunduz I, Hayes A, Waack S, Morgenstern B. 2006. AUGUSTUS: ab initio prediction of alternative transcripts. Nucleic Acids Res 34:W435–W439.

54. Simão FA, Waterhouse RM, Ioannidis P, Kriventseva E V, Zdobnov EM. 2015. BUSCO: assessing genome assembly and annotation completeness with single-copy orthologs. Bioinformatics 31:3210–3212.

55. Manni M, Berkeley MR, Seppey M, Zdobnov EM. 2021. BUSCO: Assessing genomic data quality and beyond. Curr Protoc 1:e323.

56. Johnson M, Zaretskaya I, Raytselis Y, Merezhuk Y, McGinnis S, Madden TL. 2008. NCBI BLAST: a better web interface. Nucleic Acids Res 36:W5–W9.

57. Barbeyron T, Brillet-Guéguen L, Carré W, Carrière C, Caron C, Czjzek M, Hoebeke M, Michel G. 2016. Matching the diversity of sulfated biomolecules: Creation of a classification database for sulfatases reflecting their substrate specificity. PLoS One 11:e0164846.

58. Rodriguez-R LM, Konstantinidis KT. 2016. The enveomics collection: a toolbox for specialized analyses of microbial genomes and metagenomes. PeerJ Prepr 4:e1900v1.

59. Medlar AJ, Törönen P, Holm L. 2018. AAI-profiler: fast proteome-wide exploratory analysis reveals taxonomic identity, misclassification and contamination. Nucleic Acids Res 46:W479–W485.

60. Zhang H, Yohe T, Huang L, Entwistle S, Wu P, Yang Z, Busk PK, Xu Y, Yin Y. 2018. dbCAN2: a meta server for automated carbohydrate-active enzyme annotation. Nucleic Acids Res 46:W95–W101.

688 61. Zheng J, Ge Q, Yan Y, Zhang X, Huang L, Yin Y. 2023. dbCAN3: automated
689 carbohydrate-active enzyme and substrate annotation. Nucleic Acids Res
690 51:W115–W121.

691 62. Blin K, Shaw S, Augustijn HE, Reitz ZL, Biermann F, Alanjary M, Fetter A,
692 Terlouw BR, Metcalf WW, Helfrich EJN, van Wezel GP, Medema MH, Weber
693 T. 2023. antiSMASH 7.0: new and improved predictions for detection,
694 regulation, chemical structures and visualisation. Nucleic Acids Res gkad344.

695 63. Mirdita M, Schütze K, Moriwaki Y, Heo L, Ovchinnikov S, Steinegger M. 2022.
696 ColabFold - Making protein folding accessible to all. Nat Methods 19:679–682.

697

698

699

700

Figures.

Figure 1: Phenotypic characterization of the library of filamentous microbes isolated from sediments collected along the Basque coast. A) Number of isolates obtained from each sample. See Figure 9 and Materials and Methods. B) Phenotypes of a random subset of isolates of our collection on the same culture medium (PDA, MEA, CMA, Pc or Lc) used for their isolation (see also Figure S1). The diameter of plates is 5.5 cm. (C) Classes and (D) genera represented in the subset of isolates whose ITS and/or *rpb1* regions were amplified (PCR) and Sanger-sequenced.

Figure 2: Some of the isolates staining the culture medium due to the secretion of pigments. A) Lateral view of the culture plates (left) and phenotypes of some of the isolates in MEA culture medium (right). B) Phenotype of isolate M60 in MEA (i, ii) and PDA (iii, iv) media. The diameter of plates is 5.5 cm. Developmental structures are shown in pictures v and vi. Microscopy images show germlings (vii), mature hyphae (viii), and condia formation (ix).

Figure 3: Phenotypic characterization of isolate M98. A) Phenotype of isolates M98 and M127 on minimal medium supplemented with laminarin, or fucoidan from *Fucus vesiculosus* or *Undaria pinnatifida*. Ammonium tartrate and sodium nitrate were tested as the main nitrogen source. glc: glucose; algin: alginate; lam: laminarin; fucoi: fucoidan. B) Phenotype of M98 in MEA medium (i) (5.5 cm plates), with the formation of pycnidia (ii and iii). Microscopy images show germlings (iv and v).

Figure 4: ANI analyses for isolates M60 and M98. The genomes of isolates M60 and M98 were compared to those of multiple Hypocreales species. A) ANI Matrix, and B) phylogenetic tree (BIONJ clustering method; unrooted), both generated at enveomics (http://enve-omics.ce.gatech.edu/g-matrix/index).

Figure 5: A) Predicted CAZYme repertoires of isolates M60 and M98. The graph was generated using the results given by the dbCAN website (Tables S1-S2). Three-dimensional structure prediction by ColabFold for selected glycosyl hydrolases. GH29 domains from isolates B) M60 (*M. marquandii*) and C) M98 (*A. yamanashiensis*) are shown. D) A predicted GH141 from isolate M60.

Figure 6: Number of backbone genes of secondary metabolite gene clusters predicted by antiSMASH in the genomes of M60 (A; see Figure S4) and M98 (B; see Figure S5).

Figure 7: Secondary metabolite gene clusters in the genome of isolate M60, as predicted by antiSMASH.

Figure 8: Secondary metabolite gene clusters in the genome of isolate M98, as predicted by antiSMASH.

Figure 9: Geographic location of the seven sampling points along the Basque coast selected in this work. Circles indicate estuaries while the square indicates a coastal area. EOK: river Oka; EA: river Artibai; EU: river Urola; EO: river Oria; LUR: river Urumea; EOI: river Oiartzun.

Tables.

Table 1: General data for genome sequencing analyses of isolates M60 and M98. C: Complete BUSCOs; S: Complete and single-copy BUSCOs; D: Complete and duplicated BUSCOs; F: Fragmented BUSCOs; M: Missing BUSCOs; n: Total number of BUSCOs for Hypocreales.

Isolate	**Assembly (Spades)**			**Annotation**	**BUSCO (%)**					
	Size (Mb)	***Contigs* (> 1500 bp)**	***Contigs* (all)**	**Augustus**	**C**	**S**	**D**	**F**	**M**	**n**
M60	43.69	111	461	12,946	97.1	96.1	1.0	0.5	2.4	4494
M98	31.29	44	139	10,696	97.1	96.3	0.8	0.4	2.5	4494

N50 (bp)	**N90 (bp)**	**L50**	**L90**	**Largest *contig* (bp)**
2,521,732	242,334	6	25	5,622,403
3,368,458	381,668	4	18	4,468,825

Supplementary Figures.

Figure S1: Phenotypes of a subset of 235 isolates of our library in PDA, MEA, Pc and Lc culture media, all supplemented with penicillin, grown at 25 ºC in the dark. Squares highlight isolates probably corresponding to the same strain (*e.g.*, isolates 106, 107 and 108) or different strains of the same species (*e.g.*, isolates 43, 44, 45 and 60).

Figure S2: Phenotype of selected isolates on plates filled with minimal medium supplemented with glucose, laminarin, alginate or fucoidan from *Laminaria japonica*, or without supplementation of any of these carbohydrate sources (negative control).

Figure S3: Phenotype of selected isolates on plates filled with minimal medium supplemented with 2 g/L of glucose or fucoidan from *Fucus vesiculosus* or *Undaria pinnatifida*, or without supplementation of any of these carbohydrate sources (negative control).

Figure S4: Table showing the results obtained in the analysis of the potential secondary metabolite gene clusters predicted in the genome of isolate M60 (*Marquandomyces marquandii*) by antiSMASH. The table includes the node the potential cluster is located in, the backbone enzyme(s) of each cluster, coordinates, the most similar known cluster, the type of metabolite predictably synthesized and the similarity with the reference cluster.

Figure S5: Table showing the results obtained in the analysis of the potential secondary metabolite gene clusters predicted in the genome of isolate M98 (*Albophoma yamanashiensis*) by antiSMASH.

Figure S6: Phenotype of a subset of isolates of our library in minimal medium with decreasing concentrations of bacteriological agar, without (left column) and with (right column) glucose (2 %). Considering the phenotype of the strains and solidification of the agar, a 0.5 % concentration was selected for the subsequent phenotypic characterization of the isolates.

Supplementary Tables.

773 **Table S1**: Predicted CAZYme repertoire for isolate M60. The analysis was carried out at
774 the dbCAN website (Zhang *et al.*, 2018), and the table includes the CAZYme family each
775 protein is linked to, the enzyme commission (EC) number, the tools that predicted this
776 association as well as the hypothetic presence of a signal peptide in each predicted
777 CAZYme.

778 **Table S2**: Predicted CAZYme repertoire for isolate M98.

779 **Table S3:** Genomes used as reference in ANI analyses. GenBank and BioSample
780 accession numbers are included.

781

782

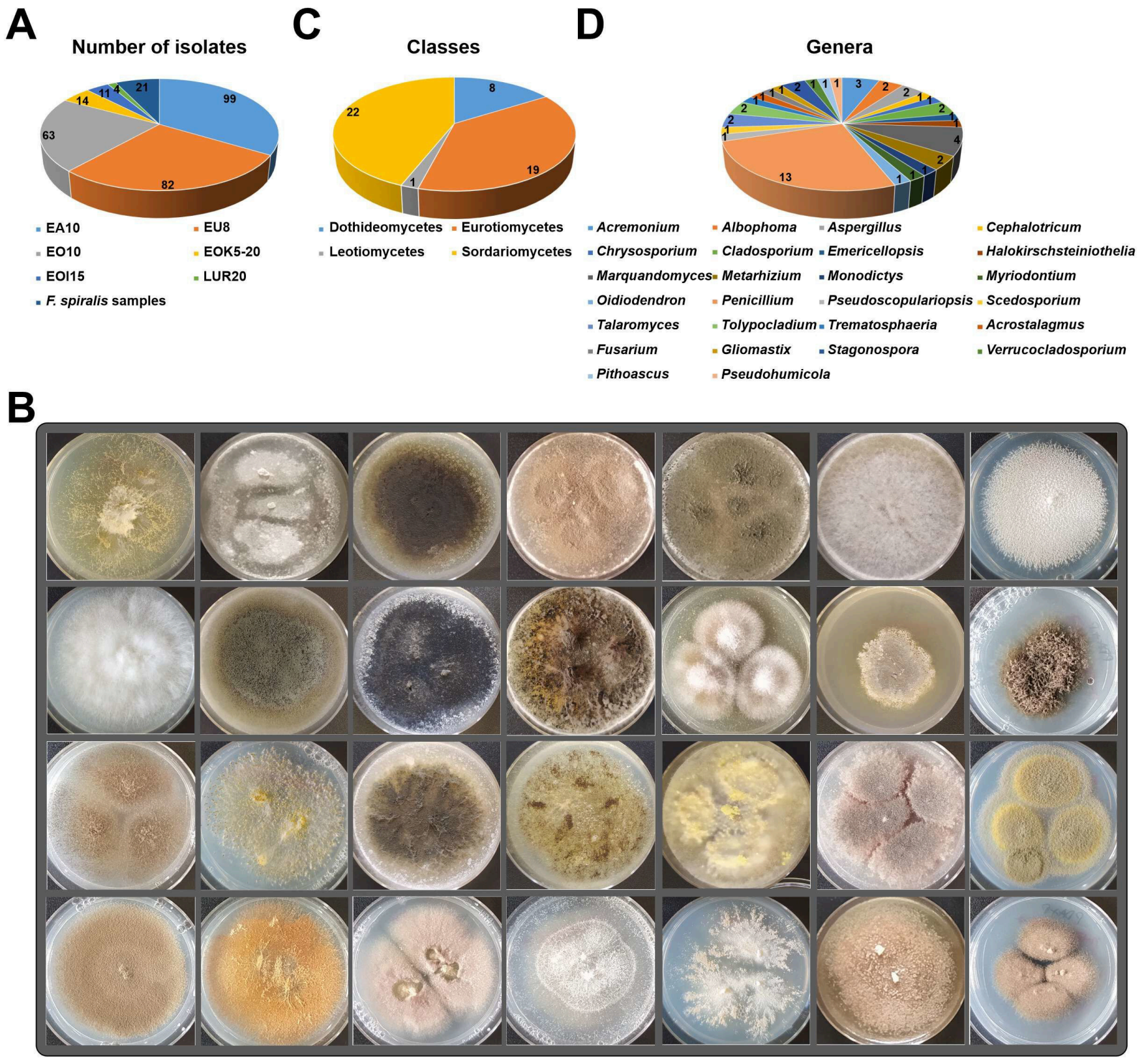
A
Number of isolates
99
82
63
14
11
4
21
EA10
EU8
EO10
EOK5-20
EOI15
LUR20
F. spiralis samples
C
Classes
8
19
1
22
Dothideomycetes
Eurotiomycetes
Leotiomycetes
Sordariomycetes
D
Genera
Acremonium
Albophoma
Aspergillus
Cephalotricum
Chrysosporium
Cladosporium
Emericellopsis
Halokirschsteiniothelia
Marquandomyces
Metarhizium
Monodictys
Myriodontium
Oidiodendron
Penicillium
Pseudoscopulariopsis
Scedosporium
Talaromyces
Tolypocladium
Trematosphaeria
Acrostalagmus
Fusarium
Gliomastix
Stagonospora
Verrucocladosporium
Pithoascus
Pseudohumicola
B

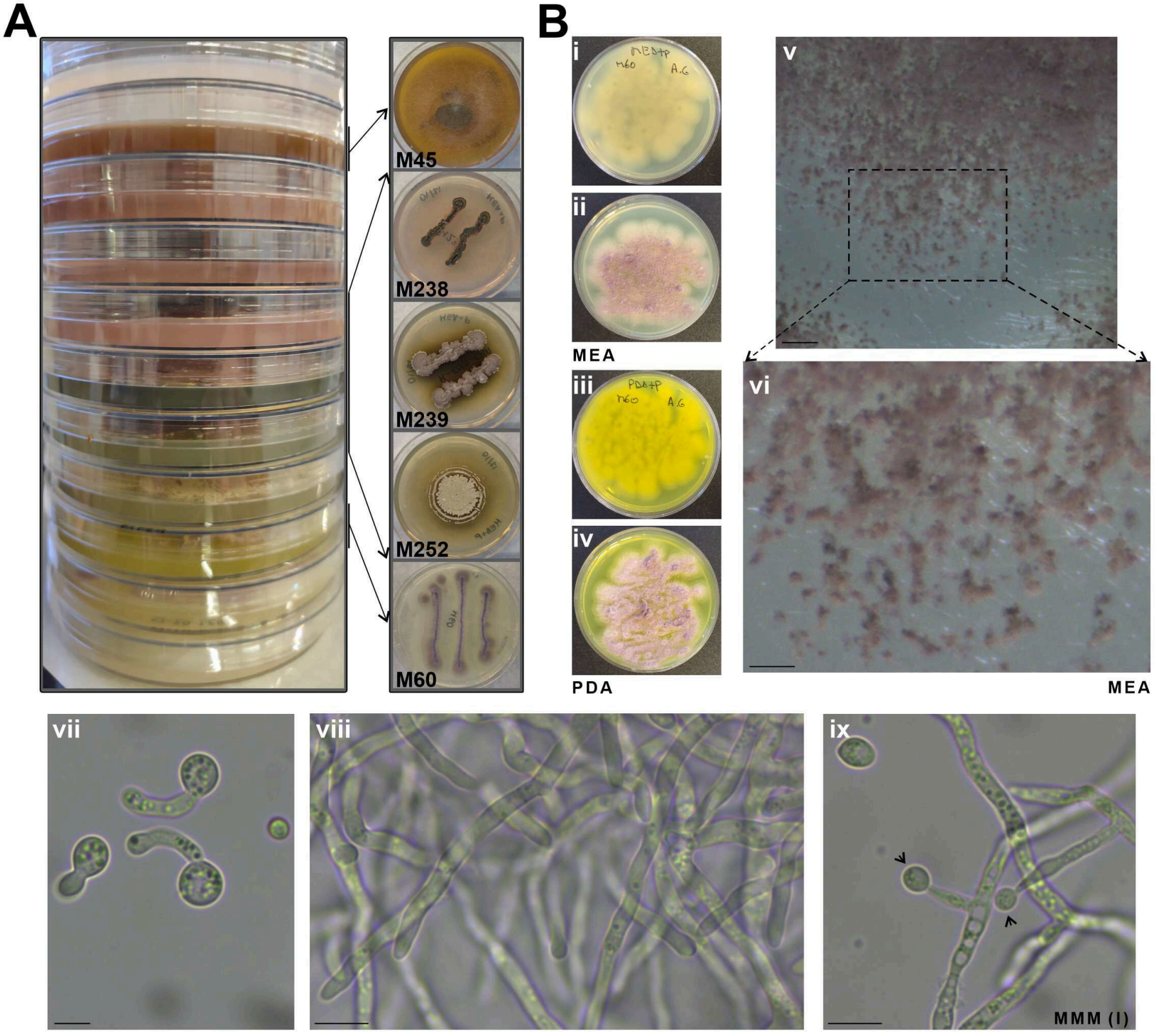
A
M45
M238
M239
M252
M60
B
i
ii
MEA
iii
iv
PDA
v
vi
MEA
vii
viii
ix
MMM (I)

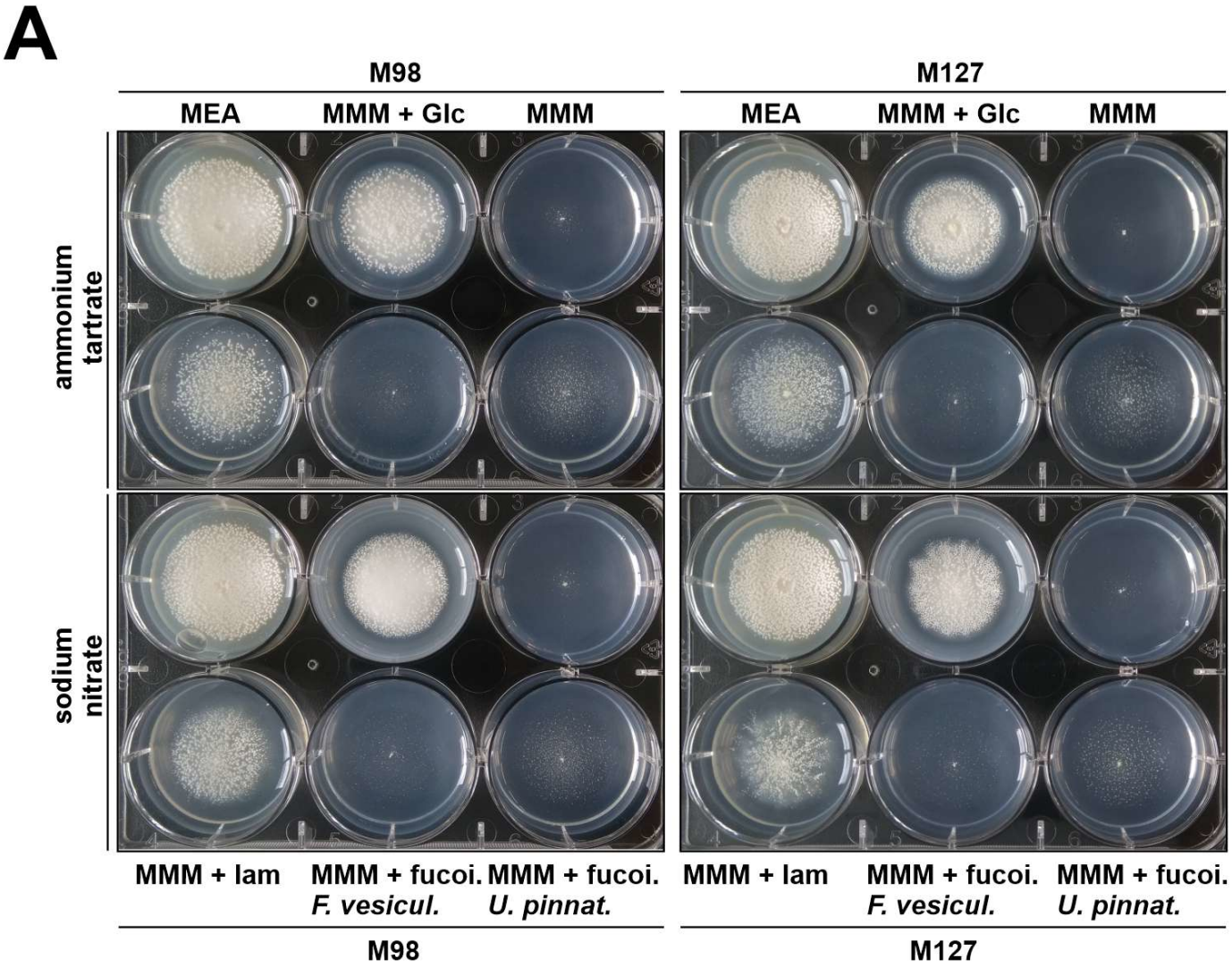
A
M98
M127
MEA
MMM + Glc
MMM
MEA
MMM + Glc
MMM
ammonium tartrate
sodium nitrate
MMM + lam
MMM + fucoi. F. vesicul.
MMM + fucoi. U. pinnat.
MMM + lam
MMM + fucoi. F. vesicul.
MMM + fucoi. U. pinnat.
M98
M127

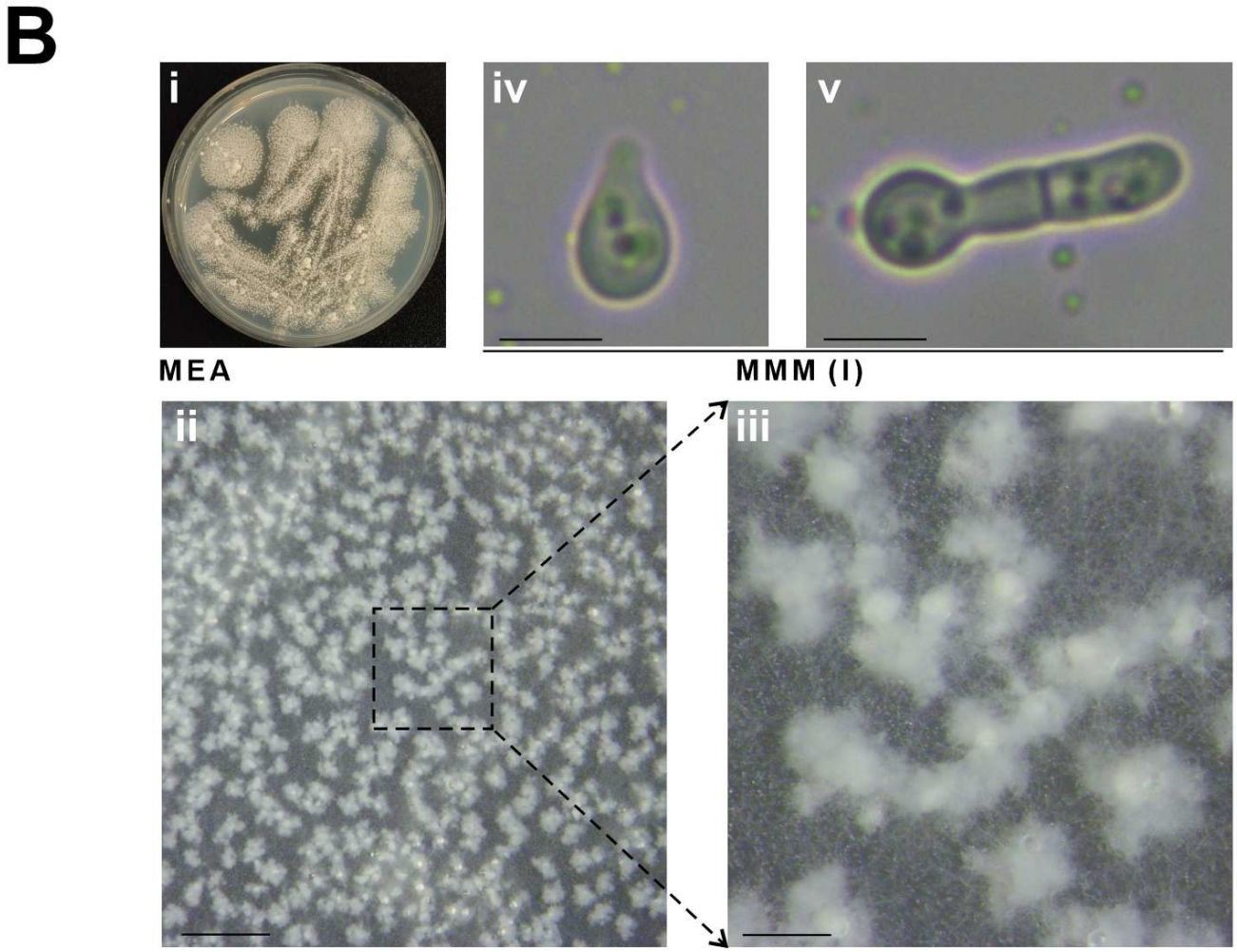
B
i
iv
v
MEA
MMM (I)
ii
iii

A

	Ophiocordyceps sinensis_1	Ophiocordyceps sinensis_2	Hirsutella rhossiliensis	Purpureocillium lilacinum_1	Purpureocillium lilacinum_2	Hirsutella thompsonii	Ophiocordyceps australis	Isolate M60	Caviceps purpurea	Ustilaginoidea virens	Drechmeria coniospora	Acremonium chrysogenum	Polycephalomyces sp.	Rugonectria rugulosa	Calonectria pseudoturangicola	Stachybotrys chartarum	Beauveria bassiana	Trichoderma reesei	Trichoderma harzianum	Neonectria coccinea	Neonectria ditissima	Fusarium oxysporum	Fusarium beomiforme	Fusarium graminearum	Metarhizium robertsii	Metarhizium anisopliae	Pochonia chlamydosporia_1	Pochonia chlamydosporia_2	Ophiocordyceps unilateralis	Ophiocordyceps camponoti-leonardi	Ophiocordyceps camponoti-floridani_1	Ophiocordyceps camponoti-floridani_2	Ophiocordyceps camponoti-rufipedis	Isolate M98	Albophoma yamanashiensis	Tolypocladium album	Tolypocladium amazonense	Tolypocladium ovalisporum	Tolypocladium guangdongense	Tolypocladium ophioglossoides	Tolypocladium paradoxum	Tolypocladium capitatum	Tolypocladium cylindrosporum	Tolypocladium inflatum
Ophiocordyceps sinensis_1	100	100	85	79	79	79	78	79	77	77	76	78	79	78	77	76	77	77	77	78	77	78	77	77	76	75	76	77	77	77	76	76	79	79	78	79	79	79	79	79	79	79	80	80	80	79	79
Ophiocordyceps sinensis_2	100	100	86	79	79	79	78	79	77	77	76	78	79	77	77	76	76	77	77	77	77	78	77	77	75	76	76	76	76	77	76	76	79	79	79	79	79	79	79	79	79	79	80	80	80	80	80
Hirsutella rhossiliensis	85	86	100	79	79	79	78	82	77	77	76	78	79	78	77	76	76	77	77	78	77	77	76	76	76	77	77	77	76	77	77	77	79	79	78	79	79	80	79	79	79	79	78	79	80	80	79	79
Purpureocillium lilacinum_1	79	79	79	100	99	86	78	79	76	78	77	78	80	78	77	77	77	78	78	79	78	78	77	78	77	77	77	77	77	77	77	77	78	79	78	78	78	80	79	79	79	79	79	80	80	80	79	79
Purpureocillium lilacinum_2	79	79	79	99	100	86	78	78	77	77	77	78	80	78	77	77	78	77	77	78	78	78	78	77	77	77	77	77	77	77	77	77	78	78	78	78	78	80	80	80	80	79	80	80	80	80	80	80
Purpureocillium takamizusanense	79	79	79	86	86	100	78	78	77	77	76	78	79	78	77	77	77	78	78	78	77	77	77	77	77	77	77	77	77	77	77	77	78	78	78	78	78	80	80	80	80	79	80	79	80	79	80	80
Hirsutella thompsonii	78	78	78	78	78	78	100	81	76	77	76	77	78	77	77	76	77	77	77	77	77	77	76	77	76	77	76	77	77	77	76	77	77	77	77	77	77	78	78	78	77	78	78	78	78	78	78	78
Hirsutella minnesotensis	79	79	82	79	78	78	81	100	76	77	76	77	78	77	77	77	77	77	77	77	77	77	77	77	77	77	77	77	77	77	77	77	78	78	78	78	78	79	78	78	78	79	78	78	78	78	79	79
Ophiocordyceps australis	77	77	77	76	77	77	76	76	100	75	75	76	77	75	75	75	75	75	76	75	76	75	75	74	74	75	76	76	75	75	75	77	77	77	77	77	77	76	76	76	76	76	76	76	77	76	76	76
Isolate M60	77	77	77	78	77	77	77	77	75	100	77	78	77	77	76	76	77	77	77	78	77	77	77	77	77	80	80	80	80	76	76	75	76	76	78	78	77	77	77	77	77	77	77	78	78	78	78	78
Caviceps purpurea	76	76	76	77	77	76	76	76	75	77	100	77	76	76	76	76	77	76	76	76	76	76	76	76	76	76	77	77	77	77	77	75	76	75	75	76	77	77	77	77	77	77	77	77	77	77	77	77
Ustilaginoidea virens	78	78	78	78	78	78	77	77	76	78	77	100	78	77	76	76	77	77	78	77	77	77	76	76	76	76	78	78	78	78	77	77	77	77	77	78	78	78	78	78	78	78	78	78	78	78	78	78
Drechmeria coniospora	79	79	79	80	80	79	78	78	77	77	76	78	100	78	77	76	77	77	77	78	77	78	77	77	77	77	77	77	77	77	77	79	79	79	79	79	80	80	79	80	79	80	79	80	80	80	80	80
Acremonium chrysogenum	78	77	78	78	78	78	77	77	75	77	76	77	78	100	76	76	77	77	78	77	77	77	77	77	77	76	77	76	77	77	77	77	77	77	77	78	78	78	78	78	78	78	78	78	78	78	78	78
Polycephalomyces sp.	77	77	77	77	77	77	77	77	75	76	76	76	76	76	100	76	76	77	76	76	76	76	76	76	76	75	76	76	76	76	76	77	76	76	76	76	77	77	77	77	77	77	77	77	77	77	77	79
Rugonectria rugulosa	76	76	76	77	77	76	77	75	76	76	76	76	76	76	76	100	78	77	77	78	78	78	78	78	78	78	77	76	77	77	76	76	76	75	75	76	77	77	77	77	77	77	77	77	77	77	77	77
Calonectria pseudoturangicola	77	76	76	77	78	77	77	77	75	77	77	77	77	77	78	100	77	77	78	78	78	78	78	78	78	78	77	77	77	77	77	76	76	76	76	76	78	77	77	77	77	77	77	77	77	77	77	77
Stachybotrys chartarum	77	77	77	78	77	77	77	77	75	77	76	77	77	77	76	77	100	77	77	77	77	77	77	77	77	77	77	77	77	77	77	77	76	76	76	76	78	78	78	77	77	77	77	77	77	77	77	78
Beauveria bassiana	77	77	77	78	77	77	77	77	75	77	76	77	77	77	76	77	77	100	77	77	77	77	77	77	77	77	77	77	77	77	77	77	76	76	76	76	77	78	77	77	77	77	77	77	77	77	77	77
Trichoderma reesei	78	77	78	79	78	78	77	77	76	77	77	78	78	78	77	77	78	77	100	82	82	78	77	77	77	77	77	77	77	77	77	77	77	77	77	79	79	78	78	78	78	78	78	78	78	78	79	79
Trichoderma harzianum	77	77	77	78	78	78	77	77	75	78	77	77	77	77	76	78	78	77	82	100	82	78	77	77	78	78	77	77	77	77	77	77	76	76	77	77	78	78	78	78	78	78	78	78	78	78	78	78
Trichoderma cornu-damae	78	78	78	78	78	78	77	77	76	77	76	77	78	77	77	77	78	77	77	82	82	100	78	77	77	76	77	77	77	77	77	77	77	77	77	77	78	78	78	78	78	79	78	78	78	78	79	78
Neonectria coccinea	77	77	77	78	77	77	77	77	75	77	76	77	77	77	76	78	78	77	77	78	78	78	100	86	78	77	77	77	77	77	76	77	76	76	76	76	78	77	77	77	77	77	78	78	78	78	77	77
Neonectria ditissima	77	77	77	78	77	77	77	77	75	77	76	76	77	77	76	78	78	77	77	77	77	77	86	100	77	77	78	77	77	76	77	76	76	76	76	76	78	78	78	78	78	77	78	78	78	78	78	78
Fusarium oxysporum	76	75	76	77	77	77	76	77	74	77	76	76	77	77	76	78	78	77	77	77	77	78	77	100	86	81	77	77	77	77	77	76	75	76	75	75	77	77	77	77	77	77	77	77	77	77	77	77
Fusarium beomiforme	75	76	76	77	77	77	77	77	74	77	77	76	77	76	76	78	78	77	77	77	78	76	77	86	100	80	77	77	77	77	77	75	75	75	75	76	77	77	77	77	76	77	76	77	76	77	76	77
Fusarium graminearum	76	76	76	77	77	77	76	77	75	77	76	76	77	75	77	78	77	77	77	78	77	77	78	81	80	100	77	77	77	76	77	75	76	75	76	76	77	77	77	77	77	77	77	77	77	77	77	77
Metarhizium robertsii	77	76	77	77	77	77	77	77	76	80	77	78	77	76	76	77	77	77	77	77	77	77	77	77	77	77	100	98	92	80	81	75	76	75	75	76	78	78	78	78	78	78	77	78	78	78	78	78
Metarhizium anisopliae	77	76	77	77	77	77	77	77	76	80	77	78	77	77	76	76	77	76	77	77	77	77	77	77	77	77	98	100	92	80	80	75	76	75	75	76	78	78	78	77	78	78	77	78	78	78	78	78
Metarhizium acridum	77	77	77	77	77	77	77	77	75	80	77	78	77	77	76	76	77	77	77	77	77	77	77	76	77	77	77	92	92	100	80	80	76	76	75	75	77	78	77	78	77	77	77	77	77	77	78	78
Pochonia chlamydosporia_1	76	76	76	77	77	77	77	77	75	80	77	78	77	77	76	77	77	77	77	77	77	77	77	77	77	76	77	77	80	80	80	100	98	75	76	75	75	76	77	77	77	77	76	76	77	77	77	77
Pochonia chlamydosporia_2	76	76	77	77	77	77	77	77	75	80	77	78	77	77	76	77	77	77	77	77	77	77	77	76	77	77	77	77	81	80	80	98	100	75	75	75	75	77	77	77	77	77	77	77	77	77	77	77
Ophiocordyceps unilateralis	79	79	79	78	78	78	77	77	77	76	75	77	79	77	76	76	76	76	77	76	77	76	77	76	76	75	75	75	76	75	75	76	75	100	82	82	82	83	78	78	78	78	78	79	78	78	79	79
Ophiocordyceps camponoti-leonardi	79	79	79	79	78	78	77	77	77	76	76	77	79	77	76	76	76	76	76	77	76	76	76	75	75	76	76	76	76	76	75	82	100	81	81	81	78	78	78	78	78	78	78	78	78	78	78	78
Ophiocordyceps camponoti-floridani_1	78	79	78	78	78	78	77	77	77	75	75	77	79	77	76	75	76	76	77	77	77	76	76	76	75	75	75	75	75	75	75	82	81	100	100	91	78	78	78	77	77	77	78	78	78	78	78	78
Ophiocordyceps camponoti-floridani_2	79	79	79	78	78	78	77	77	77	76	75	77	79	77	76	75	76	76	77	77	77	76	76	76	75	75	76	75	75	75	75	75	81	100	100	92	78	78	78	78	78	78	78	78	78	78	78	78
Ophiocordyceps camponoti-rufipedis	79	79	79	78	78	78	77	77	77	76	76	77	79	77	76	76	76	76	77	77	77	76	76	76	75	76	76	76	76	76	75	83	81	91	92	100	78	78	78	78	78	77	78	78	78	78	78	78
Isolate M98	79	79	80	80	80	80	78	78	76	78	77	78	80	78	77	77	78	77	77	79	78	78	78	78	77	77	77	78	78	77	77	78	78	78	78	78	100	99	92	88	84	84	84	84	83	84	84	84
Albophoma yamanashiensis	79	79	79	79	80	80	78	78	76	78	77	78	80	78	77	77	77	78	78	79	78	78	77	78	77	77	77	78	78	78	77	77	78	78	78	78	78	100	89	86	82	82	84	84	83	83	83	83
Tolypocladium album	79	79	79	79	80	80	78	78	76	77	77	78	79	78	77	77	77	78	77	78	78	78	77	78	77	77	77	77	78	78	77	77	78	78	78	78	92	89	100	86	83	83	84	84	83	83	83	83
Tolypocladium amazonense	79	79	79	79	80	80	78	78	76	77	77	78	80	78	77	77	77	78	77	78	78	78	77	78	77	77	77	78	78	77	77	78	78	77	78	78	88	86	86	100	83	83	84	84	83	83	83	83
Tolypocladium ovalisporum	79	79	78	79	79	79	77	78	76	77	77	78	79	78	77	77	77	77	77	78	77	78	77	78	77	76	77	78	77	77	76	77	78	78	77	78	84	82	83	83	100	83	84	84	84	83	83	83
Tolypocladium guangdongense	79	80	79	79	80	80	78	79	76	77	77	78	80	78	77	77	77	78	77	78	78	79	77	78	77	77	77	78	77	76	77	79	78	77	78	78	84	82	83	83	83	100	90	90	89	87	87	87
Tolypocladium ophioglossoides	80	80	80	80	80	79	78	78	76	77	77	78	79	78	77	77	77	77	78	78	78	78	77	77	76	77	77	77	77	77	77	78	78	78	78	78	84	84	84	84	84	90	100	90	90	89	89	89
Tolypocladium paradoxum	80	80	80	80	80	80	78	78	76	78	77	78	80	78	77	77	77	78	77	78	78	78	78	78	77	77	77	77	77	77	77	78	78	78	78	78	84	84	84	84	84	90	90	100	89	89	90	90
Tolypocladium capitatum	80	80	80	80	80	79	78	78	77	78	77	78	80	78	77	77	77	77	78	78	78	78	78	77	76	77	78	78	77	77	77	79	78	78	78	78	83	83	83	84	84	89	90	89	100	88	88	89
Tolypocladium cylindrosporum	79	80	79	79	80	80	78	79	76	78	77	78	80	78	79	77	77	78	77	79	78	79	77	78	77	77	77	78	78	78	77	77	78	78	78	78	84	83	83	83	83	87	89	89	88	100	91	91
Tolypocladium inflatum	79	80	79	79	80	80	78	79	76	78	77	78	80	78	79	77	77	78	77	79	78	78	77	78	77	77	77	78	78	78	77	77	79	78	78	78	84	83	83	83	83	87	89	90	89	91	100	100

B

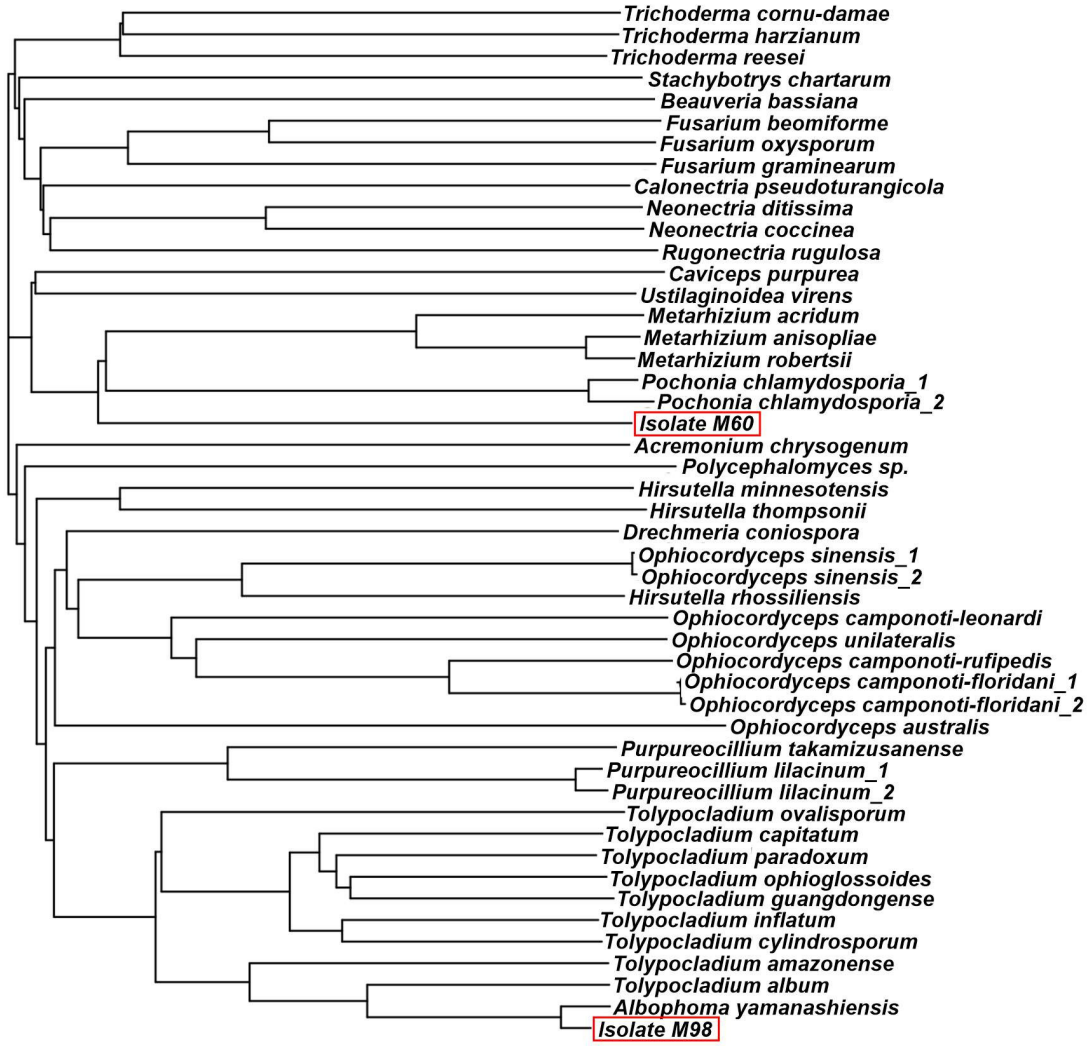

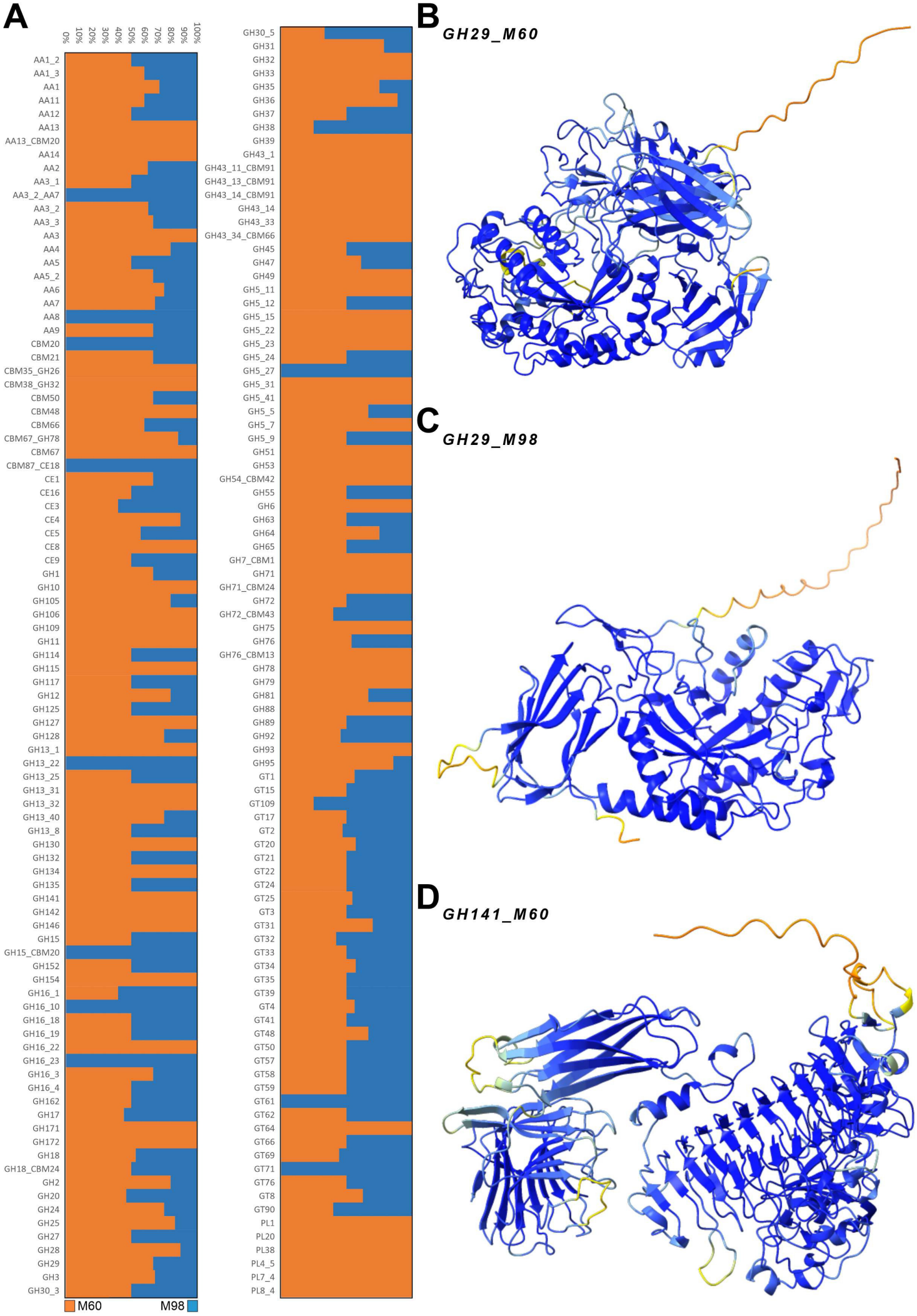
A
0%
10%
20%
30%
40%
50%
60%
70%
80%
90%
100%
AA1_2
AA1_3
AA1
AA11
AA12
AA13
AA13_CBM20
AA14
AA2
AA3_1
AA3_2_AA7
AA3_2
AA3_3
AA3
AA4
AA5
AA5_2
AA6
AA7
AA8
AA9
CBM20
CBM21
CBM35_GH26
CBM38_GH32
CBM50
CBM48
CBM66
CBM67_GH78
CBM67
CBM87_CE18
CE1
CE16
CE3
CE4
CE5
CE8
CE9
GH1
GH10
GH105
GH106
GH109
GH11
GH114
GH115
GH117
GH12
GH125
GH127
GH128
GH13_1
GH13_22
GH13_25
GH13_31
GH13_32
GH13_40
GH13_8
GH130
GH132
GH134
GH135
GH141
GH142
GH146
GH15
GH15_CBM20
GH152
GH154
GH16_1
GH16_10
GH16_18
GH16_19
GH16_22
GH16_23
GH16_3
GH16_4
GH162
GH17
GH171
GH172
GH18
GH18_CBM24
GH2
GH20
GH24
GH25
GH27
GH28
GH29
GH3
GH30_3
GH30_5
GH31
GH32
GH33
GH35
GH36
GH37
GH38
GH39
GH43_1
GH43_11_CBM91
GH43_13_CBM91
GH43_14_CBM91
GH43_14
GH43_33
GH43_34_CBM66
GH45
GH47
GH49
GH5_11
GH5_12
GH5_15
GH5_22
GH5_23
GH5_24
GH5_27
GH5_31
GH5_41
GH5_5
GH5_7
GH5_9
GH51
GH53
GH54_CBM42
GH55
GH6
GH63
GH64
GH65
GH7_CBM1
GH71
GH71_CBM24
GH72
GH72_CBM43
GH75
GH76
GH76_CBM13
GH78
GH79
GH81
GH88
GH89
GH92
GH93
GH95
GT1
GT15
GT109
GT17
GT2
GT20
GT21
GT22
GT24
GT25
GT3
GT31
GT32
GT33
GT34
GT35
GT39
GT4
GT41
GT48
GT50
GT57
GT58
GT59
GT61
GT62
GT64
GT66
GT69
GT71
GT76
GT8
GT90
PL1
PL20
PL38
PL4_5
PL7_4
PL8_4
M60
M98
B
GH29_M60
C
GH29_M98
D
GH141_M60

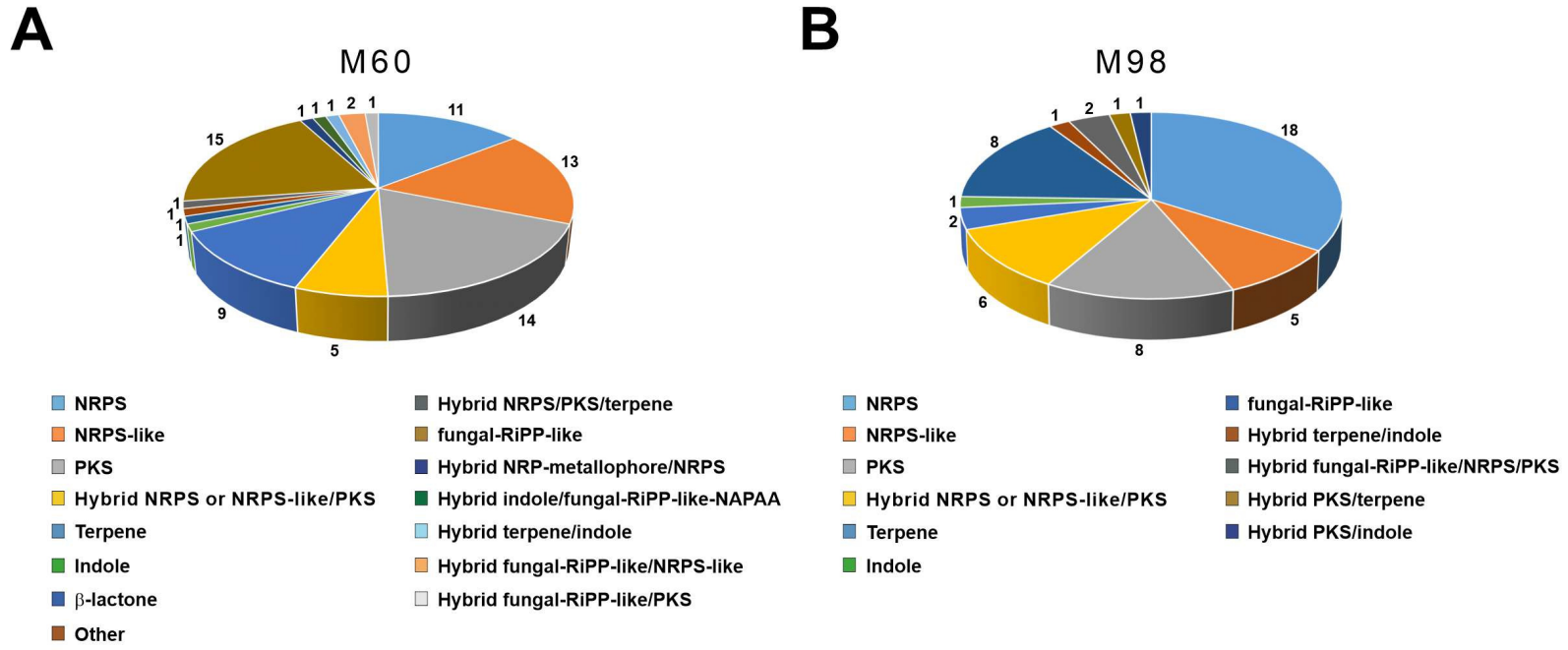
A
M60
11
13
14
5
9
15
1
1
1
1
1
1
1
1
2
1
B
M98
18
5
8
6
2
1
8
1
2
1
1
NRPS
NRPS-like
PKS
Hybrid NRPS or NRPS-like/PKS
Terpene
Indole
β-lactone
Other
Hybrid NRPS/PKS/terpene
fungal-RiPP-like
Hybrid NRP-metallophore/NRPS
Hybrid indole/fungal-RiPP-like-NAPAA
Hybrid terpene/indole
Hybrid fungal-RiPP-like/NRPS-like
Hybrid fungal-RiPP-like/PKS
NRPS
NRPS-like
PKS
Hybrid NRPS or NRPS-like/PKS
Terpene
Indole
fungal-RiPP-like
Hybrid terpene/indole
Hybrid fungal-RiPP-like/NRPS/PKS
Hybrid PKS/terpene
Hybrid PKS/indole

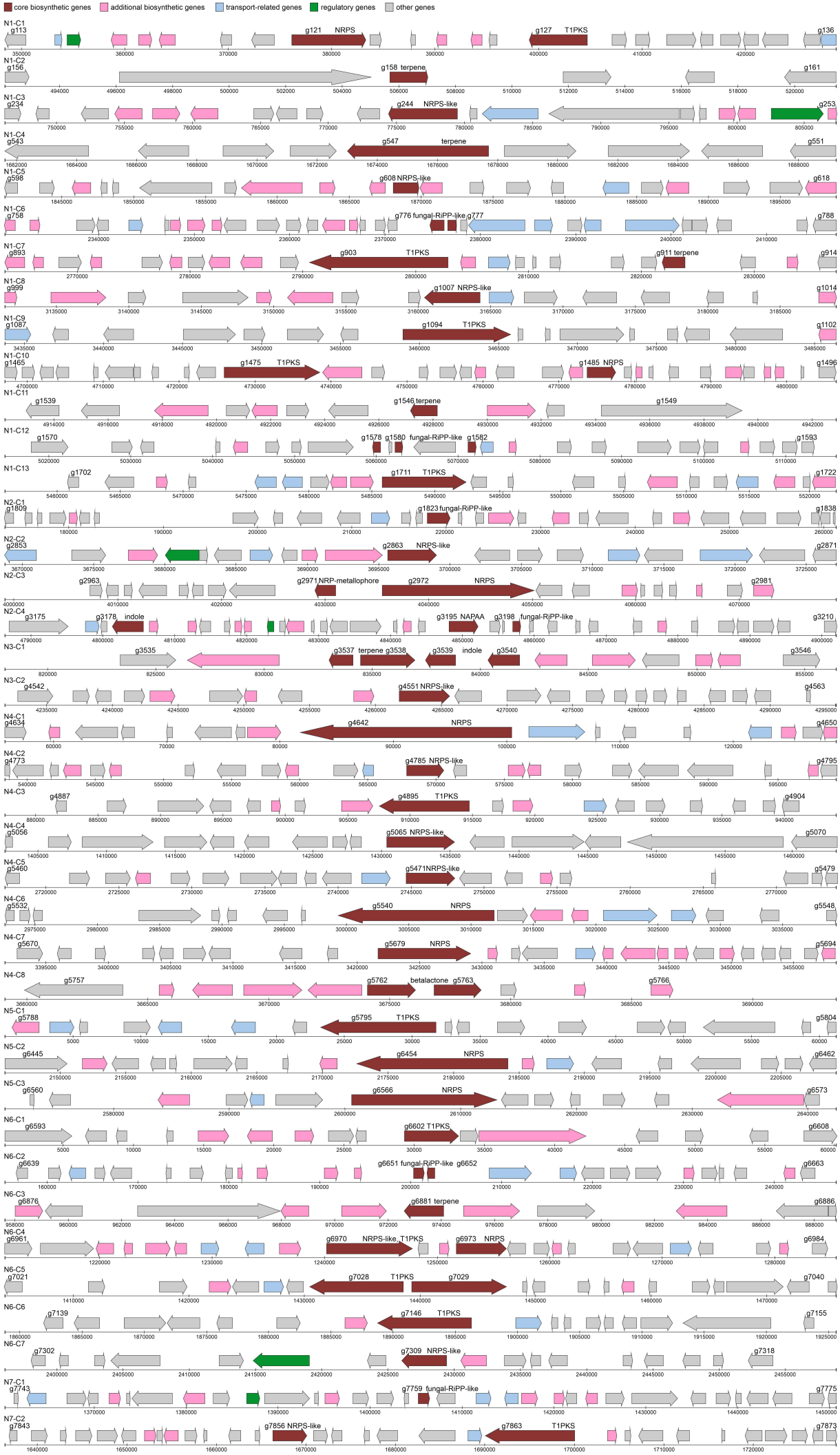
core biosynthetic genes
additional biosynthetic genes
transport-related genes
regulatory genes
other genes
N1-C1
g113
g121 NRPS
g127 T1PKS
g136
N1-C2
g156
g158 terpene
g161
N1-C3
g234
g244 NRPS-like
g253
N1-C4
g543
g547 terpene
g551
N1-C5
g598
g608 NRPS-like
g618
N1-C6
g758
g776 fungal-RiPP-like
g777
g788
N1-C7
g893
g903 T1PKS
g911 terpene
g914
N1-C8
g999
g1007 NRPS-like
g1014
N1-C9
g1087
g1094 T1PKS
g1102
N1-C10
g1465
g1475 T1PKS
g1485 NRPS
g1496
N1-C11
g1539
g1546 terpene
g1549
N1-C12
g1570
g1578
g1580 fungal-RiPP-like
g1582
g1593
N1-C13
g1702
g1711 T1PKS
g1722
N2-C1
g1809
g1823 fungal-RiPP-like
g1838
N2-C2
g2853
g2863 NRPS-like
g2871
N2-C3
g2963
g2971 NRP-metallophore
g2972 NRPS
g2981
N2-C4
g3175
g3178 indole
g3195 NAPAA
g3198 fungal-RiPP-like
g3210
N3-C1
g3535
g3537
g3538 terpene
g3539 indole
g3540
g3546
N3-C2
g4542
g4551 NRPS-like
g4563
N4-C1
g4634
g4642 NRPS
g4650
N4-C2
g4773
g4785 NRPS-like
g4795
N4-C3
g4887
g4895 T1PKS
g4904
N4-C4
g5056
g5065 NRPS-like
g5070
N4-C5
g5460
g5471 NRPS-like
g5479
N4-C6
g5532
g5540 NRPS
g5548
N4-C7
g5670
g5679 NRPS
g5694
N4-C8
g5757
g5762 betalactone
g5763
g5766
N5-C1
g5788
g5795 T1PKS
g5804
N5-C2
g6445
g6454 NRPS
g6462
N5-C3
g6560
g6566 NRPS
g6573
N6-C1
g6593
g6602 T1PKS
g6608
N6-C2
g6639
g6651 fungal-RiPP-like
g6652
g6663
N6-C3
g6876
g6881 terpene
g6886
N6-C4
g6961
g6970 NRPS-like
T1PKS
g6973 NRPS
g6984
N6-C5
g7021
g7028 T1PKS
g7029
g7040
N6-C6
g7139
g7146 T1PKS
g7155
N6-C7
g7302
g7309 NRPS-like
g7318
N7-C1
g7743
g7759 fungal-RiPP-like
g7775
N7-C2
g7843
g7856 NRPS-like
g7863 T1PKS
g7873

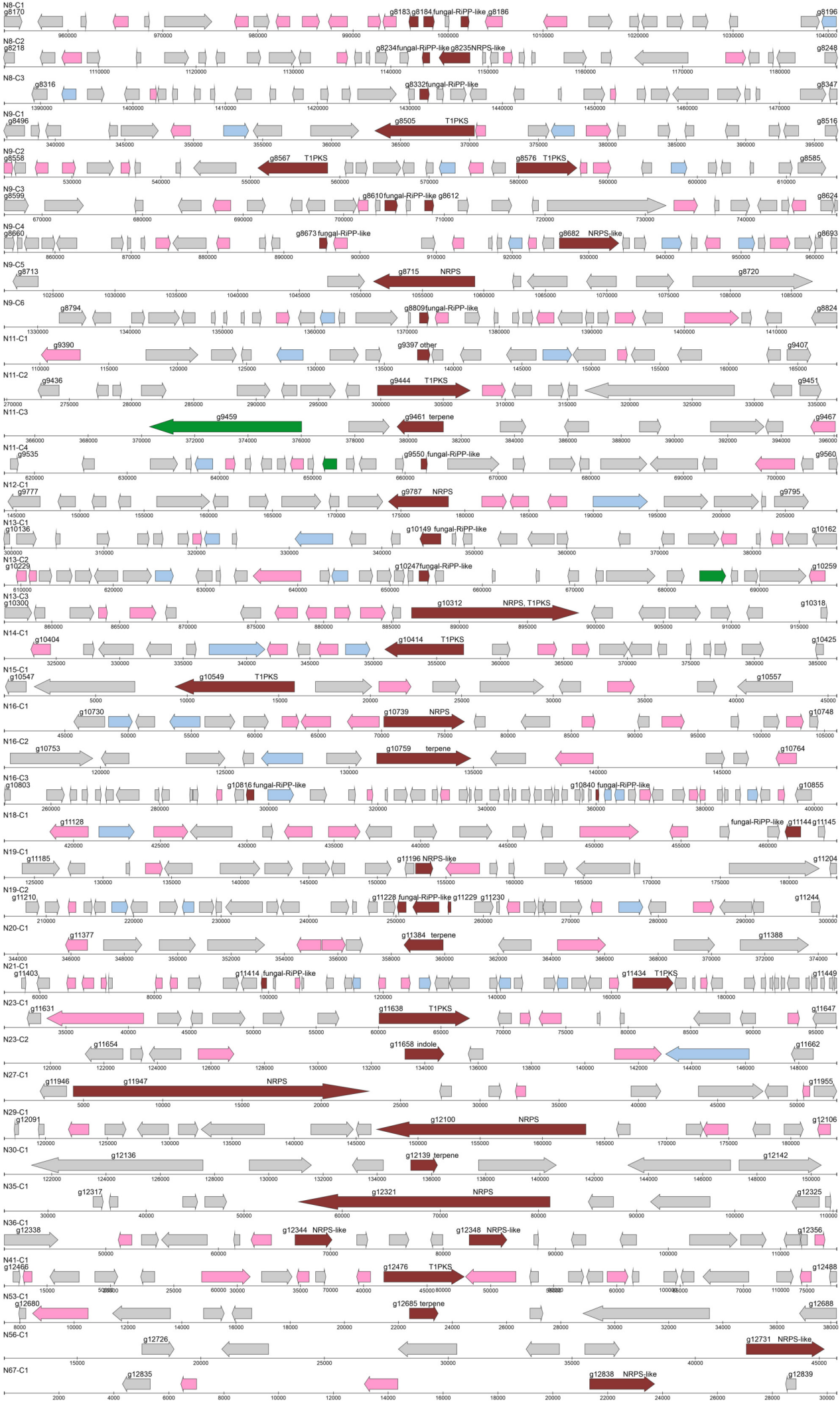
N8-C1
g8170
g8183 g8184 fungal-RiPP-like g8186
g8196
N8-C2
g8218
g8234 fungal-RiPP-like g8235 NRPS-like
g8248
N8-C3
g8316
g8332 fungal-RiPP-like
g8347
N9-C1
g8496
g8505 T1PKS
g8516
N9-C2
g8558
g8567 T1PKS
g8576 T1PKS
g8585
N9-C3
g8599
g8610 fungal-RiPP-like g8612
g8624
N9-C4
g8660
g8673 fungal-RiPP-like
g8682 NRPS-like
g8693
N9-C5
g8713
g8715 NRPS
g8720
N9-C6
g8794
g8809 fungal-RiPP-like
g8824
N11-C1
g9390
g9397 other
g9407
N11-C2
g9436
g9444 T1PKS
g9451
N11-C3
g9459
g9461 terpene
g9467
N11-C4
g9535
g9550 fungal-RiPP-like
g9560
N12-C1
g9777
g9787 NRPS
g9795
N13-C1
g10136
g10149 fungal-RiPP-like
g10162
N13-C2
g10229
g10247 fungal-RiPP-like
g10259
N13-C3
g10300
g10312 NRPS, T1PKS
g10318
N14-C1
g10404
g10414 T1PKS
g10425
N15-C1
g10547
g10549 T1PKS
g10557
N16-C1
g10730
g10739 NRPS
g10748
N16-C2
g10753
g10759 terpene
g10764
N16-C3
g10803
g10816 fungal-RiPP-like
g10840 fungal-RiPP-like
g10855
N18-C1
g11128
fungal-RiPP-like
g11144
g11145
N19-C1
g11185
g11196 NRPS-like
g11204
N19-C2
g11210
g11228 fungal-RiPP-like
g11229
g11230
g11244
N20-C1
g11377
g11384 terpene
g11388
N21-C1
g11403
g11414 fungal-RiPP-like
g11434 T1PKS
g11449
N23-C1
g11631
g11638 T1PKS
g11647
N23-C2
g11654
g11658 indole
g11662
N27-C1
g11946
g11947 NRPS
g11955
N29-C1
g12091
g12100 NRPS
g12106
N30-C1
g12136
g12139 terpene
g12142
N35-C1
g12317
g12321 NRPS
g12325
N36-C1
g12338
g12344 NRPS-like
g12348 NRPS-like
g12356
N41-C1
g12466
g12476 T1PKS
g12488
N53-C1
g12680
g12685 terpene
g12688
N56-C1
g12726
g12731 NRPS-like
N67-C1
g12835
g12838 NRPS-like
g12839

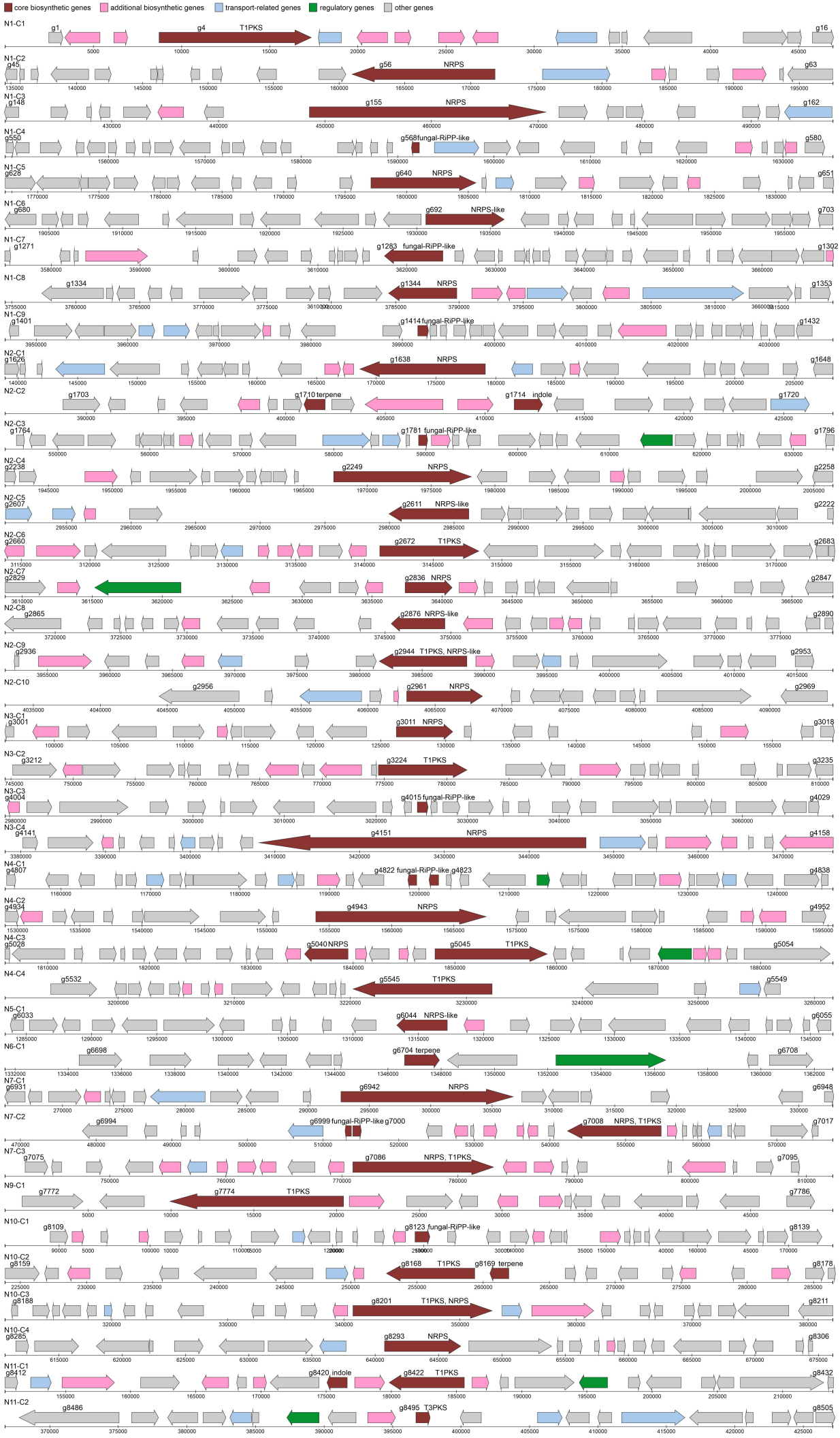
core biosynthetic genes
additional biosynthetic genes
transport-related genes
regulatory genes
other genes
N1-C1
g1
g4 T1PKS
g16
N1-C2
g45
g56 NRPS
g63
N1-C3
g146
g155 NRPS
g162
N1-C4
g550
g568 fungal-RiPP-like
g580
N1-C5
g628
g640 NRPS
g651
N1-C6
g680
g692 NRPS-like
g703
N1-C7
g1271
g1283 fungal-RiPP-like
g1302
N1-C8
g1334
g1344 NRPS
g1353
N1-C9
g1401
g1414 fungal-RiPP-like
g1432
N2-C1
g1626
g1638 NRPS
g1648
N2-C2
g1703
g1710 terpene
g1714 indole
g1720
N2-C3
g1764
g1781 fungal-RiPP-like
g1796
N2-C4
g2238
g2249 NRPS
g2258
N2-C5
g2607
g2611 NRPS-like
g2222
N2-C6
g2660
g2672 T1PKS
g2683
N2-C7
g2829
g2836 NRPS
g2847
N2-C8
g2865
g2876 NRPS-like
g2890
N2-C9
g2936
g2944 T1PKS, NRPS-like
g2953
N2-C10
g2956
g2961 NRPS
g2969
N3-C1
g3001
g3011 NRPS
g3018
N3-C2
g3212
g3224 T1PKS
g3235
N3-C3
g4004
g4015 fungal-RiPP-like
g4029
N3-C4
g4141
g4151 NRPS
g4158
N4-C1
g4807
g4822 fungal-RiPP-like
g4823
g4838
N4-C2
g4934
g4943 NRPS
g4952
N4-C3
g5028
g5040 NRPS
g5045 T1PKS
g5054
N4-C4
g5532
g5545 T1PKS
g5549
N5-C1
g6033
g6044 NRPS-like
g6055
N6-C1
g6698
g6704 terpene
g6708
N7-C1
g6931
g6942 NRPS
g6948
N7-C2
g6994
g6999 fungal-RiPP-like
g7000
g7008 NRPS, T1PKS
g7017
N7-C3
g7075
g7086 NRPS, T1PKS
g7095
N9-C1
g7772
g7774 T1PKS
g7786
N10-C1
g8109
g8123 fungal-RiPP-like
g8139
N10-C2
g8159
g8168 T1PKS
g8169 terpene
g8178
N10-C3
g8188
g8201 T1PKS, NRPS
g8211
N10-C4
g8285
g8293 NRPS
g8306
N11-C1
g8412
g8420 indole
g8422 T1PKS
g8432
N11-C2
g8486
g8495 T3PKS
g8505

N11-C3
g8538
g8548 T1PKS
g8555
525000 530000 535000 540000 545000 550000 555000 560000 565000 570000 575000 580000 585000 590000
N12-C1
g8724
g8733 T1PKS
g8743
415000 420000 425000 430000 435000 440000 445000 450000 455000 460000 465000 470000 475000
N15-C1
g9189
g9198 NRPS
g9208
70000 75000 80000 85000 90000 95000 100000 105000 110000 115000 120000 125000 130000
N15-C2
g9227
g9235 NRPS
g9245
190000 195000 200000 205000 210000 215000 220000 225000 230000 235000 240000
N15-C3
g9258
g9266 NRPS, T1PKS
g9284 fungal-RiPP-like g9285
g9299 fungal-RiPP-like
g9323 T1PKS
300000 320000 340000 360000 380000 400000 420000 440000 460000 480000
N16-C1
g9420
g9431 NRPS
g9442
290000 295000 300000 305000 310000 315000 320000 325000 330000 335000 340000 345000 350000
N17-C1
g9523
g9527 indole
g9531
130000 135000 140000 145000 150000 155000
N18-C1
g9665
g9678 NRPS
g9688
130000 140000 150000 160000 170000 180000 190000 200000
N21-C1
g10016
g10026 NRPS
g10035 NRPS
g10047
80000 90000 100000 110000 120000 130000 140000 150000 160000 170000 180000 190000 200000
N23-C1
g10211
g10217 terpene
g10223
178000 180000 182000 184000 186000 188000 190000 192000 194000 196000 198000 200000 202000 204000 206000 208000
N24-C1
g10257
g10266 NRPS
g10272
90000 100000 110000 120000 130000 140000 150000 160000
N25-C1
g10294
g10302 NRPS-like
g10309
25000 30000 35000 40000 45000 50000 55000 60000 65000 70000 75000 80000 85000
N31-C1
g10533
g10543 g10545 fungal-RiPP-like g10549 g10550
g10569
10000 20000 30000 40000 50000 60000 70000 80000
N34-C1
g10607
T1PKS
g10616
5000 10000 15000 20000 25000 30000 35000 40000

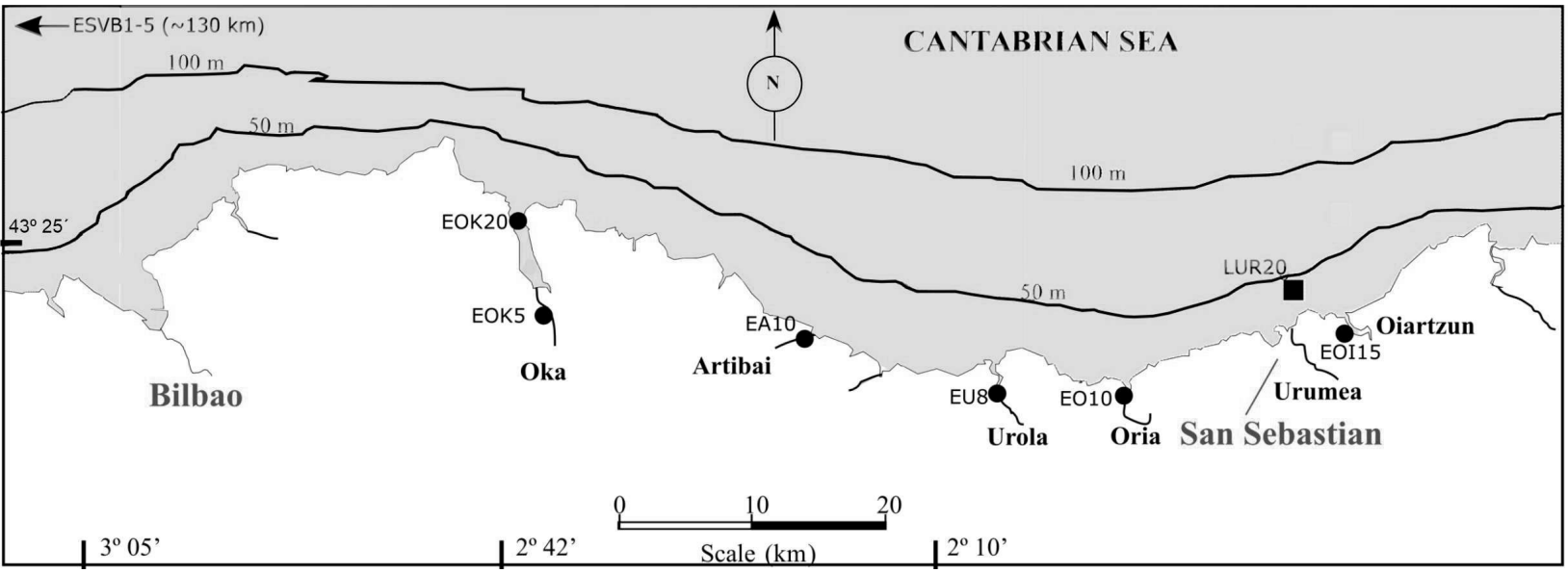
ESVB1-5 (~130 km)
CANTABRIAN SEA
N
100 m
50 m
100 m
50 m
43º 25´
EOK20
EOK5
Oka
Bilbao
EA10
Artibai
EU8
Urola
EO10
Oria
LUR20
Oiartzun
EOI15
Urumea
San Sebastian
0
10
20
Scale (km)
3º 05'
2º 42'
2º 10'